

إقرار

أنا الموقع أدناه مقدم الرسالة التي تحمل العنوان :

تصميم هوائي الرقعة للتطبيقات ذات النطاق العريض

Design a Microstrip Patch Antenna for Ultra Wide Band (UWB)

Applications

أقر بأن ما اشتملت عليه هذه الرسالة إنما هي نتاج جهدي الخاص ، باستثناء ما تمت الإشارة إليه حيثما ورد ، وإن هذه الرسالة ككل ، أو أي جزء منها لم يقدم من قبل لنيل درجة أو لقب علمي أو بحثي لدى مؤسسة تعليمية أو بحثية أخرى.

DECLARATION

The work provided in this thesis, unless otherwise referenced, is the researcher's own work, and has not been submitted elsewhere for any other degree or qualification.

اسم الطالب: سامر عمر حسان عودة Student's name: SAMER O. H. OUDA

Signature: 

التوقيع: 

Date: 02/01/2013

التاريخ: 02/01/2013

The Islamic University Of Gaza

Faculty of Graduate Studies

Department of Communication Systems Engineering



Master Thesis

Design a Microstrip Patch Antenna for Ultra Wide Band (UWB) Applications

Advisors:

Dr. Mohamed Ouda

Dr. Mustafa Abu Nasr

Prepared by:

Samer Omar Ouda

120090500

A thesis submitted for the Master of Science degree in Electrical Engineering



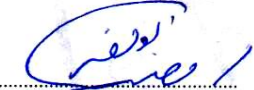
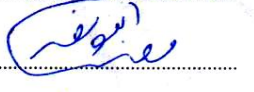


نتيجة الحكم على أطروحة ماجستير

بناءً على موافقة عمادة الدراسات العليا بالجامعة الإسلامية بغزة على تشكيل لجنة الحكم على أطروحة الباحث/ سامر عمر حسان عودة لنيل درجة الماجستير في كلية الهندسة قسم الهندسة الكهربائية - أنظمة اتصالات وموضوعها:

تصميم هوائي الرقعة للتطبيقات ذات النطاق العريض

Design a Microstrip Patch Antenna for Ultra Wide Band (UWB) Applications

وبعد المناقشة التي تمت اليوم الأربعاء 20 صفر 1434هـ، الموافق 2013/01/02م الساعة الواحدة ظهراً، اجتمعت لجنة الحكم على الأطروحة والمكونة من:

	مشرفاً ورئيساً	د. محمد خليل عودة
	مشرفاً	د. مصطفى حسن أبو نصر
	مناقشاً داخلياً	د. فادي إبراهيم النحال
	مناقشاً خارجياً	د. يوسف العبد حمودة

وبعد المداولة أوصت اللجنة بمنح الباحث درجة الماجستير في كلية الهندسة/ قسم الهندسة الكهربائية - أنظمة اتصالات.

واللجنة إذ تمنحه هذه الدرجة فإنها توصيه بتقوى الله ولزوم طاعته وأن يسخر علمه في خدمة دينه ووطنه.

والله ولي التوفيق،،،

عميد الدراسات العليا

د. فؤاد علي العاجز
أ.د. فؤاد علي العاجز

Abstract

The development of Ultra Wide Band (UWB) technology, including antennas as an essential part of wireless communication systems, is greatly accelerated. However, there are more challenges in designing a UWB antenna more than a narrow band one. It should be capable of operating over an ultra-wide bandwidth as allocated by the Federal Communications Commission (FCC) from 3.1GHz to 10.6GHz. At the same time, the radiation properties over the entire frequency range are also necessary to be satisfactory.

This thesis focuses on a designing a novel microstrip Ultra Wide Band (UWB) antenna for optimum performance like wide bandwidth, good matching impedance, small antenna size exhibits a good voltage standing wave ratio (VSWR) performance and its E- and H-plane radiation patterns are stable over the UWB frequency range and others. This antenna has a new patch shape that allows for providing good properties. Discussing the necessary parameters of UWB antennas, and studying the techniques of enhancing the bandwidth of a microstrip UWB are also investigated, to get antenna exhibit excellent performance of UWB characteristics with enhanced bandwidth.

The first antenna studied in this thesis is a microstrip star-shape antenna which is a new shape and we call it (SSA) by using Ansoft's HFSS software package. The antenna consists of a star-shape radiating element with a partial ground plane and a microstrip line feed from the edge of the patch. Feeding patch from edge consider as a method for enhancing the bandwidth as we will see later. The parameters structure of the antenna was optimized to achieve the widest antenna bandwidth and impedance matching.

A parameter study was conducted to optimize antenna parameters. It helps to investigate the effect of different parameters on the impedance bandwidth. So our study are also includes studding the effect of feed line shift of microstrip line from center of patch to its edge and shows how it plays an important role with enhancing the bandwidth and reaches it to 18.6GHz (from 3.9GHz to 22.5GHz). Also the effect of the ground plane length is studied and shows how it

serves as an impedance matching circuit and also it tunes the resonant frequencies. The effect of feed line width is also investigated.

The second antenna studied is a slotted star shape antenna which has new ground plane shape. It consists of partial ground plane with multiple rectangular slots at top side of ground. This is another method for enhancing the bandwidth. Also the effect of the length and width of slots was studied, and shows how it has opposite effect on return loss value.

The impedance bandwidth of this antenna is enhanced and reaches 20.6 GHz (3.9 GHz to 24.5 GHz).

The properties of antenna namely; bandwidth, input impedance, radiation pattern and VSWR, were investigated for both antennas and show how we get good results for both .

Acknowledgments

I would like to express my most sincere gratitude to my supervisor, Professor Mohammad Ouda for his guidance, support and encouragement. His big experience and deep understanding of the subject of my thesis helped me a lot to walk in the right direction in the study process, and also his minute notes and observations in many things have helped in this research excellence.

A special acknowledgement goes to my second supervisor, Professor Mustafa Abu Nasr who was the main backer for me who guided me significantly and continuously in every step. He was the source of information research that I needed and, that was useful and well-focused on the subject of the thesis. I thank him for his scientific and practical inputs that were given to me during the study period.

I am also grateful to Dr. Ammar Abo hadrouss and Dr. Hala al Kozondar who reviewed the proposal and development of important notes.

I would also like to acknowledge the Department of Electronic Engineering in the Islamic University of Gaza, for the financial support.

I cannot finish without mentioning my great parents, and my dear wife who have been offering all round support during the period of my study.

CONTENTS

Abstract	i
Acknowledgments	iii
Table of Contents	iv
List of Figures	viii
Chapter 1 Introduction	
1.1 Introduction	1
1.2 Motivation	2
1.3 Organization of The Thesis	4
Chapter 2 Antenna Fundamentals	
2.1 Introduction	5
2.2 Radiation Pattern	6
2.2.1 Radiation Pattern Lobes	7
2.2.2 Isotropic, Directional, and Omni-directional Patterns.	8
2.3 Characterization of Antenna	9
2.3.1 Directivity	9
2.3.2 Antenna Efficiency	10
2.3.3 Gain	12
2.3.4 Bandwidth	12
2.4 Polarization	13
2.4.1 Linear Polarization	13

2.4.2 Circular Polarization	14
2.4.3 Elliptical Polarization	14
2.5 Input Impedance	15
2.6 Microstrip Patch Antenna	17
2.7 Basic Characteristics	18
2.7.1 Feeding Techniques	19
2.7.1.1 Microstrip Feed Line	20
2.7.1.2 Coaxial Feed /Probe Coupling	20
2.7.1.3 Aperture-Coupled Feed	21
2.7.1.4 Proximity-Coupled Feed	22
2.8 Microstrip Transmission Line	22
2.9 Microstrip Transmission Line Matching	25
2.9.1 Inset Feed	26
2.9.2 Quarter-Wave Transformer	27
Chapter 3 UWB Antennas and Finite Element Method	
3.1 UWB Antenna Characteristic	29
3.2 Types of UWB Antenna	30
3.2.1 Travelling Wave Antennas	30
3.2.2 Frequency Independent Antennas	31
3.2.3 Small Element Antennas	32
3.2.4 Multi-Resonant Antennas	34
3.3 Numerical Solution	34
3.3.1 Review of Electromagnetic Theory	34

3.3.1 Finite Element Method (FEM)	36
3.3.1.1 Solving Differential Equation Using FEM for One Dimension	36
3.4 Literature Review and Methodology	38
Chapter 4 UWB Star Shape Antennas	
4.1 Introduction	43
4.2 Antenna Structure	43
4.3 Simulation Setup and Result	44
4.3.1 Antenna Return loss and Bandwidth	44
4.3.2 Antenna Input Impedances	45
4.3.3 Antenna Gain	47
4.3.4 Antenna Radiation Pattern	48
4.3.5 VSWR	50
4.4 Parameters Study	50
4.4.1 Effect of Feed Shift(Offset Feed)	50
4.4.2 Effect of the Ground Plane Length	53
4.4.3 Effect of The Feed Line Width	54
4.5 SSA With Slotted Ground Plane	55
4.6 Antenna Structure	55
4.7 Simulation Setup and Result	56
4.7.1 Antenna Return Loss and Bandwidth	56
4.7.2 Antenna Input Impedances	57
4.7.4 Antenna Radiation Pattern	58

4.7.5 VSWR	59
4.8 Parameters Study	59
4.8.1 Effect of Slots Width	59
4.8.2 Effect of Slots Length	60
Chapter 5 Conclusions and Future Work	
5.1 Conclusion	62
5.2 Suggestions for Future Work	63
References	64

List of Figures

Figure (2.1): Antenna as a transition device	5
Figure (2.2): Convenient set of coordinates	6
Figure (2.3): pattern achieves its half power using graphs with different scales	7
Figure (2.4): Major, minor, side, and back lobes	8
Figure (2.5): Antenna efficiencies	11
Figure (2.6): Linear polarization	13
Figure (2.7): Circular polarization	14
Figure (2.8): Elliptical polarization	15
Figure (2.9): Equivalent circuit of antenna	16
Figure (2.9-a): Top view of patch antenna	18
Figure (2.9-b): Side view of patch antenna	18
Figure (2.10): Electric field distribution on patch antenna	18
Figure (2.11): Common shapes of microstrip patch elements	19
Figure (2.12): Microstrip feed line	20
Figure (2.13): Coaxial cable feed of patch antenna	21
Figure (2.14): Aperture coupled feed.	21
Figure (2.15): Proximity coupled Feed	22
Figure (2.16): Microstrip line	22
Figure (2.17): Electric field line	23
Figure (2.18): Patch antenna with an inset feed.	26
Figure (2.19): Patch antenna with a quarter-wavelength matching section	27

Figure (3.1): Horn antenna	31
Figure (3.2): LTSA, Vivaldi, CWSA and, BLTSA	31
Figure (3.3): Spiral, log periodic, conical spiral and logarithmic spiral antenna antennas	32
Figure (3.4): Monopole, biconical, single core, and, bow-tie antennas	33
Figure (3.5): Different plate shape	33
Figure (3.6): Division of irregular domain in to triangular	36
Figure (3.7): The Finite element method for one dimensional	37
Figure (3.8): One- dimensional FEM approximation	37
Figure (3.9): Patch with single slot and partial ground plane	39
Figure (3.10): Antenna with small cut on the outskirts of patch	39
Figure (3.11): Antenna with partial ground plane with multiple rectangular slot at top side	40
Figure (3.12): Antenna with an etched slot at the lower edge and vertical slot on the patch and a small cut on the ground5	40
Figure (3.13): Antenna with additional external patch on back side of the substrate (a)Top view (b) bottom and side view.	41
Figure (3.14): Structure of partial slotted ground antenna with addition of stair and stubs	41
Figure (3.15): Antenna with symmetrical single-beveled planar patch with rectangular shaped slot and partial ground plane.	42
Figure (3.16): Patch antenna with EBG	42
Figure (4.1): Star shape antenna	44
Figure (4.2): Return loss for SSA	45
Figure (4.3): Antenna impedance	45
Figure (4.4): 50Ω microstrip line	46
Figure (4.5): Quarter-wavelength transformer for microstrip line	47
Figure (4.6): Resistance R and reactance X	47

Figure (4.7): The simulated of maximum Gain at $\phi = 0^\circ, 90^\circ$ over frequency band	48
Figure (4.7-a): E-plane at 10.2GHz, $\phi = 0^\circ$	48
Figure (4.7-b): H-plane at 10.19GHz, $\theta = 90^\circ$	48
Figure (4.7-c): E-plane at 17.8GHz, $\phi = 0^\circ$	49
Figure (4.7-d): H-plane at 17.8GHz, $\theta = 90^\circ$	49
Figure (4.7-e): Y-Z plane at 17.8GHz, $\phi = 90^\circ$	49
Figure (4.7-f): Y-Z plane at 10.2GHz, $\phi = 90^\circ$	49
Figure (4.8): VSWR for SSA	50
Figure (4.9): Simulated return loss curves of different feed shift	51
Figure (4.10-a): Resistance R	52
Figure (4.10-b): Reactance X	52
Figure (4.11): Feed shift steps for microstrip line with current distribution on patch	53
Figure (4.12): Simulated return loss curve of different ground plan length	53
Figure (4.13): Variation of bandwidth with wf	54
Figure (4.14): SSA with rectangular slots on ground plane	55
Figure (4.15): Dimension of rectangular slot	56
Figure (4.16): Return loss of antenna with and without slot	56
Figure (4.17): Resistance R and reactance X	57
Figure (4.18-a): Radiation pattern at x-z plane, $\phi = 0^\circ$	58
Figure (4.18-b): Radiation pattern at x-y, $\theta = 90^\circ$	58
Figure (4.18-c): Radiation pattern at y-z, $\phi = 90^\circ$	58
Figure (4.19): VSWR for slotted antenna	59

Figure (4.20): Variation of RL with for different ($ws = 0.42\text{mm}, 0.84\text{mm}, 1.26\text{mm}, 1.68\text{mm}$) 60

Figure (4.21): Variation of RL with different ($ls = 0.167\text{mm}, 0.334\text{mm}, 0.501\text{mm}, 0.67\text{mm}$) 61

Chapter 1

Introduction

1.1 Introduction

Ultra Wide Band (UWB) communication system was able to put foundation stone to different approaches of wireless communications system. In 1886 Heinrich Hertz proved Maxwell's equation and made the first spark gap transmission. The first UWB communication system was started in London in 1896 and was linking two post offices at a distance greater than one mile[1]. Modern UWB appeared in 1960 when the U.S. military used pulse transmissions for hiding imaging, radar and stealth communications [2].

The main advantage of UWB system is that, according to Shannon-Hartley theorem, channel capacity is in proportion to bandwidth. Since UWB has an ultra wide frequency bandwidth, it can achieve huge capacity as high as hundreds of Mbps. Also UWB systems operate at extremely low power transmission levels, so due to these properties it can provide highly secure and highly reliable communication solutions due to the low energy density which makes unintended detection quite difficult. Lastly, UWB system based on impulse radio features low cost and low complexity which arise from the essentially baseband nature of the signal transmission [3].

In February, 2002, the FCC amended the Part 15 rules which govern unlicensed radio to include the operation of UWB devices. The FCC also allocated a bandwidth of 7.5GHz, i.e. from 3.1GHz to 10.6GHz to UWB applications. According to the FCC's ruling, any signal that occupies at least 500MHz spectrum can be used in UWB systems. That means UWB is not

restricted to impulse radio any more, it also applies to any technology that uses 500MHz spectrum and complies with all other requirements for UWB.

UWB systems are based on impulse radio because it transmitted data at very high data rates by sending pulses of energy rather than using a narrow band frequency carrier. Normally, the pulses have very short durations, typically a few nanoseconds (billionths of a second) that results in an ultra-wideband frequency spectrum [3].

There are many different applications for UWB, one of them is that used for Low Data Rate (LDR) applications such as very simple transmitters that prohibit the use of energy significantly which allows the battery to long life. This is mainly used in low data rate networks like that used in military applications that are difficult to detect, and also excel in jamming resistance. Another application used in UWB is the one used for High Data Rate (HDR) applications like, internet access and multimedia services, Location-based services, and home networking and home electronics [4].

1.2 Motivation

The maximum achievable data rate or capacity for the ideal band-limited additive is related to the bandwidth and signal-to-noise ratio (SNR) by Shannon-Nyquist criterion, as shown in Equation (1.1)

$$C = B \log_2(1 + SNR) \quad (1.1)$$

where C denotes the maximum transmit data rate, B stands for the channel bandwidth. From the equation above we can see that the data rate can be increased by increasing the transmission power or the bandwidth occupation. However, the transmit's power can't readily be increased because all portable devices are battery-powered. Thus, a large frequency bandwidth will be the solution to achieve high-data rate.

The above equation also indicates that channel capacity increases linearly with bandwidth and decreases logarithmically as the SNR decreases. This relationship suggests that channel capacity can be enhanced more rapidly by increasing the occupied bandwidth than the SNR. Thus, for

wireless personal area network that only transmits over short distances, where signal propagation loss is small and less variable, greater capacity can be achieved through broader bandwidth occupancy.

UWB technology can be considered as one of the most promising wireless technologies that promises to revolutionize high data rate transmission with low power and, enables the personal area networking industry leading to new innovations and greater quality of services to the end users. For that UWB system experienced many significant developments in recent years[3]. Design of UWB antenna is still the main challenge and it's one of the challenges in making this technology live up to its full potential. Among the classical broadband antenna configurations that are under consideration for use in UWB systems is a horn antenna which provides high bandwidth but has a large size [5] and is not suitable for indoor applications. A Vivaldi antenna is a directional antenna and is not suitable for indoor and portable devices. A straight wire monopole antenna is a simple structure, but its bandwidth is very low [3]. So we found that there is a great effort to provide a small size and low cost UWB antenna that provides satisfactory performances of UWB system and has the ability to provide wide bandwidth to improve channel capacity by increased bandwidth occupancy.

Microstrip antenna (also known as a patch antenna) is one of the latest technologies in antennas and electromagnetic applications. It's used widely in the wireless communication system due to its simplicity and compatibility with printed circuit technology [6]. It provides high data rate transmission, light weight, low volume and, low fabrication cost, however it has a narrow bandwidth [7]. The bandwidth of antenna enhanced using different techniques as we will show later.

In this thesis, new microstrip star-shaped antennas (SSA) are designed and studied. (SSA) antenna is investigated in detail in order to understand its operation, find out the mechanism that leads to the UWB characteristic and also obtain some quantitative guidelines for designing this type of antenna. The new antennas will provide large bandwidths and satisfy the requirements of UWB antenna applications. Also, good properties were obtained by modifying the ground plane shape.

1.4 Organization of The Thesis

This thesis is organized in five chapters as follows:

Chapter 2: This chapter covers the fundamental antenna theory. The microstrip antennas are also discussed, the feeding type and, matching techniques are also represented

Chapter 3: A brief introduction to UWB technology is presented in this chapter. The primary requirements for a suitable UWB antenna are discussed. Also different types of UWB antenna are represented. A brief introduction of numerical solution and finite element method is described. The literature review and methodology are also investigated .

Chapter 4: In this chapter, a microstrip star- shape antenna(SSA) is designed and studied. A parameter study was conducted to optimize antenna parameters. These parameters are: - shift of feed line, ground plane length, and feed line width. Also the modification of ground plane shape was studied

Chapter 5: Conclusion and future work are given in this chapter.

Chapter 2

Antenna Fundamentals

2.1 Introduction

An antenna can be considered as important part in any wireless communication system. It can be defined as a metallic device that is used to radiate or receive radio wave. The transmit antennas used to radiate electromagnetic waves into free space and receive antenna are used to collect radiation from free space and deliver the energy contain in radio wave to the guiding device then to receiver. So the antenna is the transitional structure between free-space and a guiding device, as shown in figure (2.1). There is different form of guiding device or transmission line. It may be coaxial line or waveguide and it is used to transport electromagnetic energy from the transmitting source to the antenna or from the antenna to the receiver.

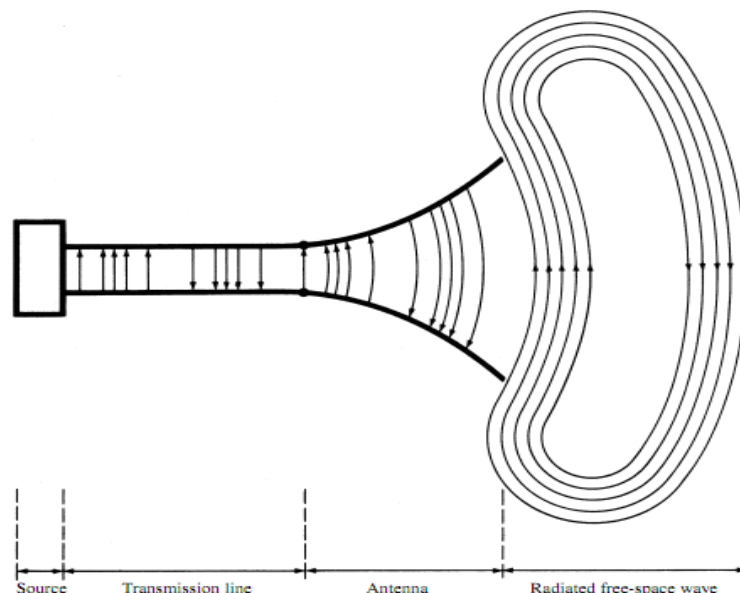


Figure (2.1): Antenna as a transition device [6].

There are various parameters to describe the performance of antenna. In this chapter some of these parameters will be defined which is considered an important parameter that given a full description of antenna [6].

2.2 Radiation Pattern

Radiation pattern or antenna pattern can be defined as graphical or mathematical function that represents the radiation properties of the antenna. It is determined in far field region and it includes power flux density, radiation intensity, field strength, directivity, phase or polarization. The **Amplitude field pattern** can be consider as received electric (magnetic) field at a constant radius of sphere that the antenna is placed in the middles of sphere. The variation of the power density along a constant radius is called an **Amplitude power pattern**. Graphical representations of radiation pattern are also represented as a function of space coordinates, a convenient set of coordinates is shown in figure(2.2)[6].

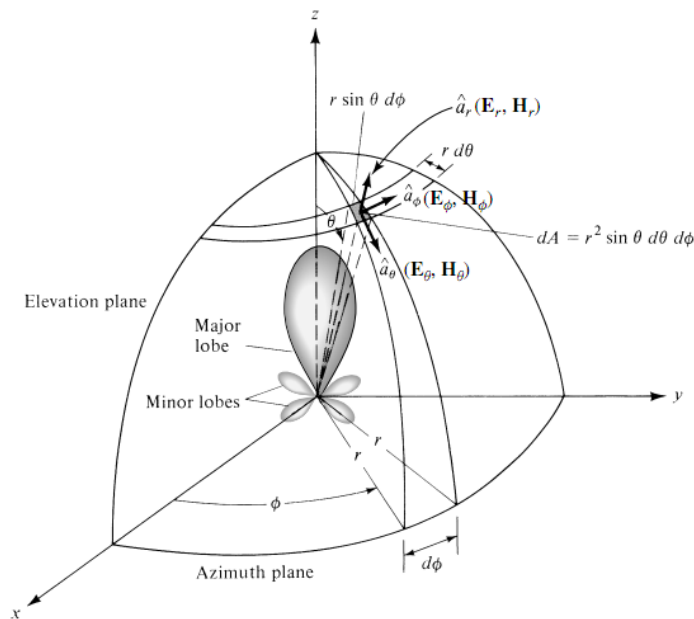


Figure (2.2): Convenient set of coordinates [6].

To find the points where the pattern achieves its half power using graphs with different scales as shown in figure(2.3) below, relative to the maximum value of the pattern, set the value of the two-dimensional normalized field pattern (plotted in linear scale), power pattern(plotted in linear scale), and power pattern (plotted on a log arithmetic dB scale) to :

- Field pattern at 0.707 value of its maximum, as shown in figure(2.3-a)
- Power pattern (in a linear scale) at its 0.5 value of its maximum, as shown in figure (2.3-b)
- Power pattern (in dB) at -3 dB value of its maximum, as shown in figure (2.3-c)[6].

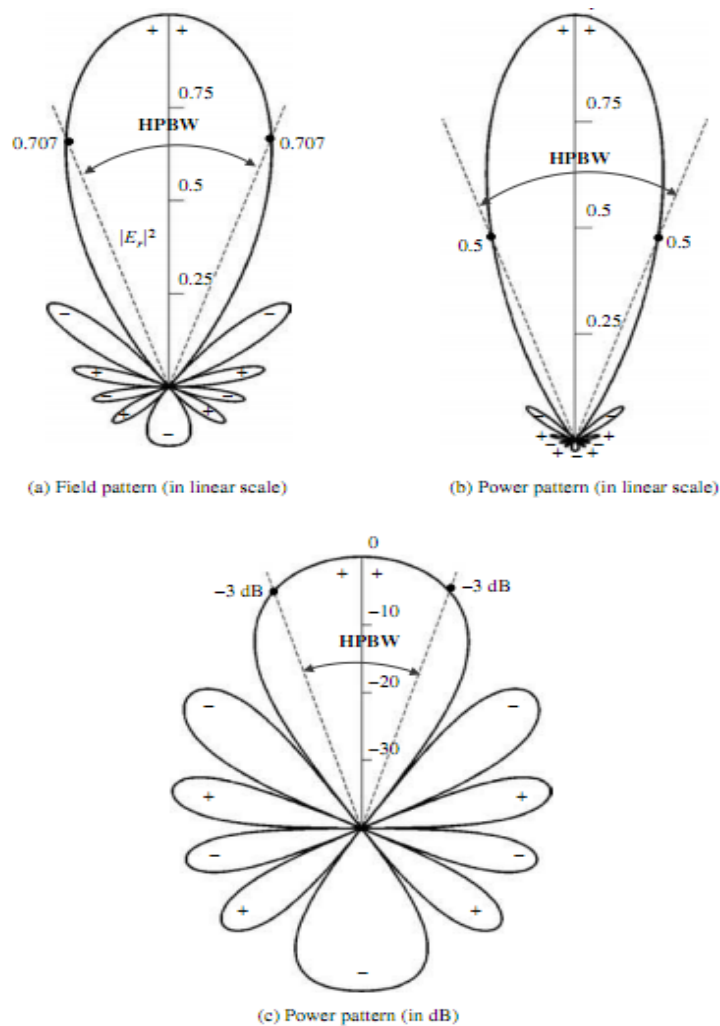


Figure (2.3): Pattern achieves its half power using graphs with different scales[6].

2.2.1 Radiation Pattern Lobes

A radiation lobe may be sub-classified into major or main, minor, side, and back lobes. figure (2.4-a) demonstrates a symmetrical three-dimensional polar pattern with a number of radiation lobes. Some are greater radiation intensity than others, but all are classified as lobes. figure(2.4-b) illustrates linear two-dimensional pattern where the same pattern characteristics are indicated.

The radiation lobe that contains the direction of maximum radiation is called **Major lobe** or main beam and, the **Minor lobe** is any lobe except a major lobe. The radiation lobe in any direction other than the intended lobe refers to **Side lobe**. Usually a side lobe is adjacent to the main lobe and occupies in same direction of the main beam. A **back lobe** is a radiation lobe whose axis makes an angle of approximately 180° with respect to the beam of an antenna. Usually it refers to a minor lobe that occupies in a direction opposite to that of the major (main) lobe. Undesired radiation is represented by Minor lobes and is usually in undesired directions, and they should be minimized. Side lobes are normally the largest of the minor lobes[6].

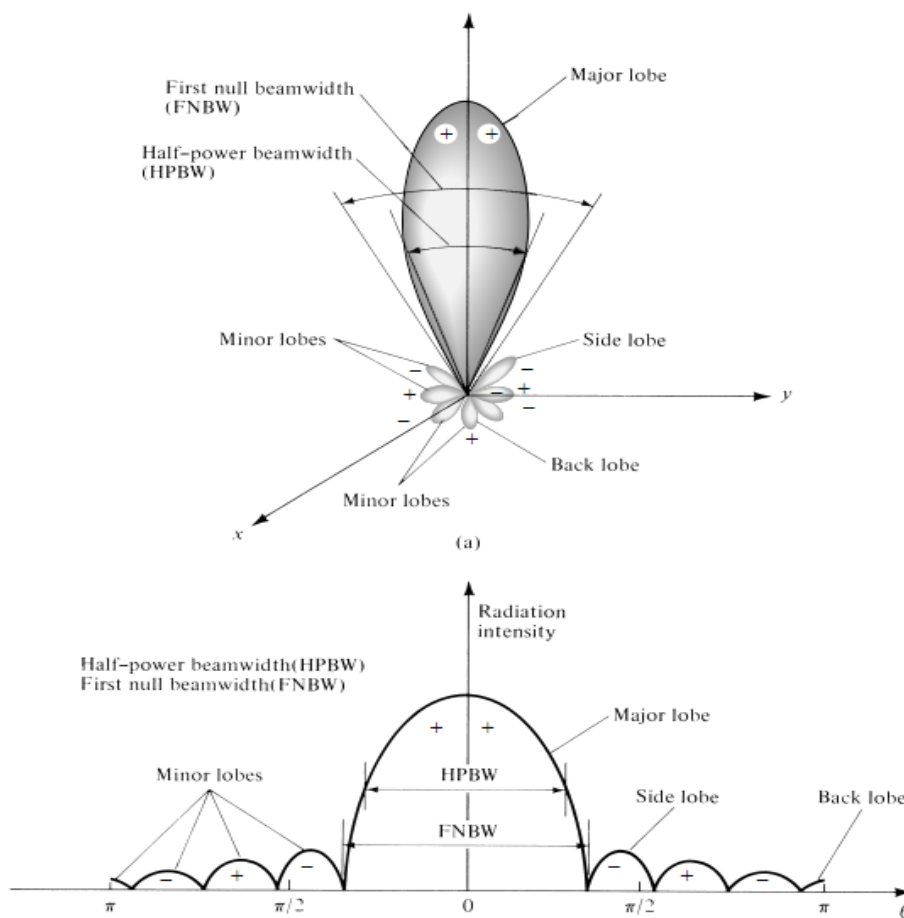


Figure (2.4):Major, minor, side, and back lobes [6]

2.2.2 Isotropic, Directional, and Omni-directional Patterns

An **isotropic radiator** is defined as; a lossless antenna that has equal radiation patterns in all directions. It's an ideal radiator and is not found in real life but it is often taken as a reference for expressing the directive properties of actual antennas. A **directional antenna** is one that has

directional properties that can radiate or receive electromagnetic waves in some direction more effectively than another. **Omni-directional**, defined as one having an essentially non-directional pattern in a given plane and a directional pattern in any orthogonal plane. An Omni-directional pattern is then a special type of a directional pattern [6].

2.3 Characterization of Antenna

The electromagnetic wave is radiated by antenna and carried power away from antenna. Pointing vector represented the power density of a wave. The pointing vector for a sinusoidal time varying field is given by equation (2.1)

$$\overline{P_{avg}} = \frac{1}{2} \text{Re} \{ \overline{E} X \overline{H}^* \} \quad (2.1)$$

$\overline{P_{avg}}$ is the time average power density in watt per square meter (W / m^2) it's a vector whose direction point in the direction of point of propagation. \overline{H}^* denotes complex conjugate of the magnetic field. The total average power radiated is given by integral of $\overline{P_{avg}}$ over an appropriate surface, S as show in equation (2.2)

$$P_{rad} = \frac{1}{2} \iint_s \text{Re} \{ \overline{E} X \overline{H}^* \} . ds \quad (2.2)$$

let P_{avg} be magnitude of the pointing vector. Since far field have $1/r$ dependency, the quantity that presented in equation (2.3)

$$U = r^2 P_{avg} \quad (2.3)$$

U is called the radiation intensity and, in general, is a function of angle ϕ and θ [8].

2.3.1 Directivity

The ability of antenna to focus radiation is described by the term of directivity. It can be used to measure directivity properties of antenna compared with an isotropic antenna defined as the ratio of radiation intensity in specific direction from antenna to radiation intensity of isotropic antenna and, it can introduced mathematically using equation (2.4)

$$D = \frac{U}{U_o} \quad (2.4)$$

For isotropic source the power is equal in all directions so the radiation intensity for isotropic source can be expressed as shown in equation (2.5)

$$U_o = \frac{P_{rad}}{4\pi} \quad (2.5)$$

where P_{rad} is total radiator power, so the directivity becomes as show in equation (2.6)

$$D = \frac{4\pi U}{P_{rad}} \quad (2.6)$$

where D , U , U_o , is directivity, radiation intensity and, radiation intensity of isotropic antenna respectively. If the direction is not specified the directivity can be defined as the ratio of maximum radiation intensity to radiation intensity of isotropic antenna as show in equation (2.7) below[8].

$$D_{max} = \frac{U_{max}}{U_o} = \frac{4\pi U_{max}}{P_{rad}} \quad (2.7)$$

2.3.2 Antenna Efficiency

The ability of antenna to transmit input power to radiation is called antenna efficiency. So it can be describable as the ratio between radiated powers to input power as shown in equation (2.8) below

$$e = \frac{P_{rad}}{P_{in}} \quad (2.8)$$

Different type of efficiencies can be found. The multiplication of all these efficiencies is called total antenna efficiency. figurer (2.5) below can be used to define a number of antenna efficiencies. The antenna efficiency can be effected by lossless at the input terminal due to reflection that occurs from the mismatch between the transmission line and the antenna as shown in figure (2.5-a) and, within structure of antenna, such losses (conduction and dielectric) as shown in figure (2.5-b).

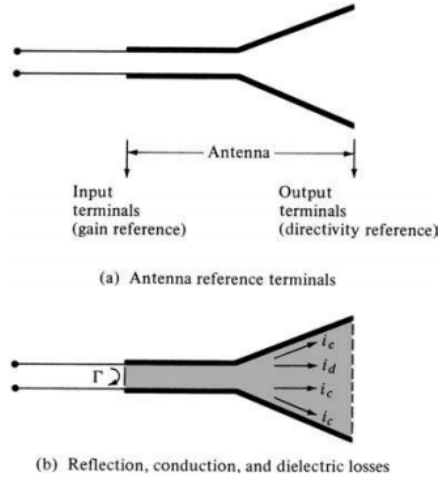


Figure (2.5): Antenna efficiencies[6]

Reflection efficiency occur from mismatch between the transmission line and the antenna and can be calculate from equation (2.8)

$$e_r = 1 - \Gamma^2 \quad (2.8)$$

where Γ is voltage reflection coefficient at the input terminals of the antenna and can be found from equation (2.9)

$$\Gamma = \frac{z_{in} - z_o}{z_{in} + z_o} \quad (2.9)$$

where z_{in} and z_o is antenna input impedance and, characteristic impedance of the transmission line respectively. e_c , e_d are difficult to compute and it can be determined experimentally. It usually cannot be separated and it is related to antenna radiation efficiency $e_{cd} = e_c e_d$ which is related to conduction losses and dielectric losses. In general, the total antenna efficiency can be written as shown in equation (2.10)

$$e_o = e_r e_c e_d = e_r e_{cd} \quad (2.10)$$

where e_o, e_r, e_c and e_d are total efficiency, reflection efficiency conduction efficiency and, dielectric efficiency respectively and all these quantity are dimensionless[6].

2.3.3 Gain

Another important parameter which describe the properties of antenna is the gain. Gain is quantity that is related to the directivity. It is defined as the ratio between maximum radiation intensity to the input power as shown in equation (2.11)

$$G = \frac{4\pi U_{\max}}{P_{in}} \quad (2.11)$$

The difference between gain and directivity is the power using in equation. For a lossless antenna the radiated power is equal to input power $P_{rad}=P_{in}$. Another difference between gain and directivity is measurement of gain that takes into account the efficiency of antenna because the radiated power is equal to the input power minus dissipated power due to losses, so the ratio of radiated power to the input power is expressed as shown in equation (2.12)

$$P_{rad} = e_{cd} P_{in} \quad (2.12)$$

where e_{cd} is placed in range $0 \leq e_{cd} \leq 1$, so can the gain be expressed as shown in equation (2.13) below

$$G = \frac{4\pi U_{\max}}{P_{in}} = e_{cd} \frac{4\pi U_{\max}}{P_{rad}} = e_{cd} D \quad (2.13)$$

but the directivity is taking into account only the directional properties of the antenna and is therefore controlled only by the pattern[8].

2.3.4 Bandwidth

Bandwidth can be defined as the operation frequency rang that the antenna performance respects to some characteristic performs as desired. Also the bandwidth can be related to frequency band that the radiation pattern doesn't change within this band. For broadband antenna the bandwidth can be defined as the ratio between upper to lower frequencies as shown in equation (2.14)

$$BW = \frac{f_H}{f_L} \quad (2.14)$$

where f_H and, f_L is upper and lower frequency respectively. For narrowband antenna the bandwidth can be expressed as a percentage of frequency difference between upper and lower frequency over center frequency f_c as shown in equation (2.15) below[9].

$$BW = 200 \frac{f_H - f_L}{f_c} \% \quad (2.15)$$

2.4 Polarization

The orientation of antenna is play an important role in transmitted and received operation. A single wire antenna will have one polarization if it is mounted vertically to the earth and it will have different polarization if it is mounted horizontally to the earth. So the definition of polarization is, orientation of electric field of transmitted or received wave with respect to the earth and how it's determined with orientation of antenna [9].

2.4.1 linear Polarization

Figure (2.6) below represents a linear polarization which is defined, for a time harmonic wave, as the propagation wave that assumes linear polarization at given point if the electric or magnetic field vector is always orientated at the same straight line at that given point at every instant of time. This is occurring if there is only one component or there are two components that are in phase or 180° (or multiples of 180°) out of phase. In linear polarization the antenna compels emitted wave for particular orientation depending on the orientation of antenna mounting. The usual cause is horizontal and vertical polarization [6].

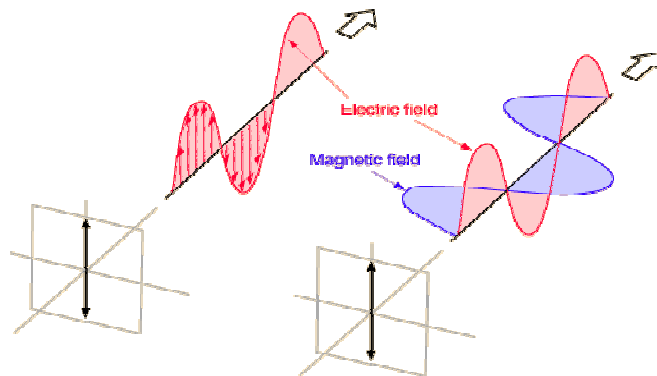


Figure (2.6) Linear polarization[10]

2.4.2 Circular Polarization

For a time harmonic wave, the propagation wave is said to be circular polarization at a given point if the electric or magnetic field vector traces a circle as a function of time. The electric field is continuously varying through all possible values of its orientation with time as shown in figure (2.7). This occurs if the field has two orthogonal linear components and the two components must have the same magnitude and it must have a time-phase difference of odd multiples of 90° . There is a right-hand (or clockwise) circularly polarized wave and,

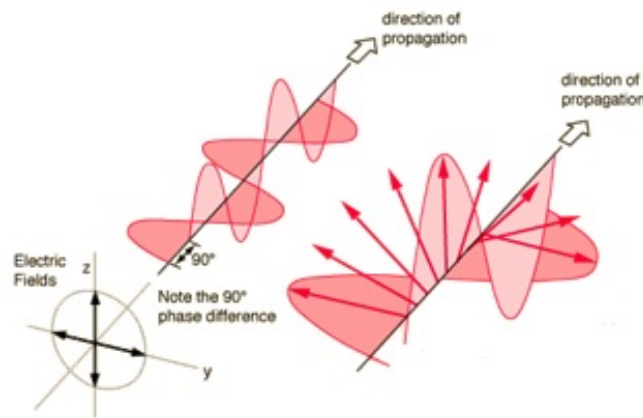


Figure (2.7): Circular polarization [10]

a left-hand (or counterclockwise) circularly polarized wave. If the wave travels away from an antenna and its rotation is clockwise, the wave is right-hand circularly polarized and if the wave travels away from an antenna and its rotation is counterclockwise, the wave is left-hand circularly polarized[6].

2.4.3 Elliptical Polarization

For a time harmonic wave, the propagation wave is said to be elliptical polarization at a given point if the electric or magnetic field traces an elliptical path in space as shown in figure (2.8). The wave is right-hand elliptical polarized if its rotation is clockwise and, the wave is left-hand elliptical polarized if its rotation is counterclockwise. Circular and linear polarization is a special case of elliptical polarization. The wave is elliptically polarized if it is not circularly or linearly

polarized. The elliptical polarization can occur if the field has two orthogonal linear components and the two components can have the same or different magnitude[6].

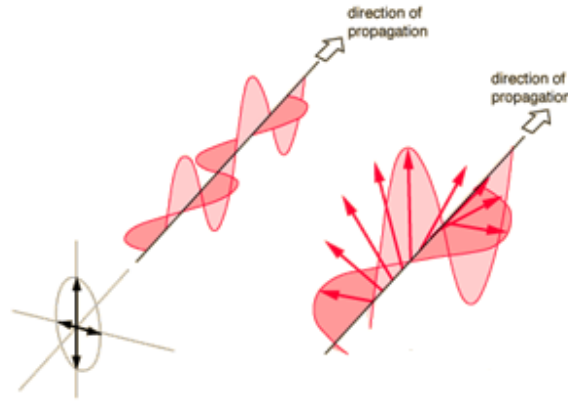


Figure (2.8): Elliptical polarization[10]

2.5 Input Impedance

Until electromagnetic wave travel in different parts of the antenna system they faced different impedance in each interface. The electromagnetic waves travel from source to transmission line to antenna then to free spaces. They encounter mismatch impedance at each interface and cause some of these waves to reflect back to the source forming a standing wave in transmission line. Standing Wave Ratio (SWR) is a ratio of maximum power to a minimum power. An SWR 1:1 is ideal. To minimize SWR it must minimize impedance mismatch between each interface at each part of the antenna system which allows to maximum power transfer to each part until it reaches antenna then free spaces. Input Impedance Z_{in} of antenna can be defined as the frequency response of an antenna at its port. Also it is the ratio between the voltage and current at the antenna port. It is complex quantity that is functioning with frequency as shown in equation (2.16).

$$Z_{in}(f) = R_{in}(f) + jX_{in}(f) \quad (2.16)$$

where Z_{in} , R_{in} , X_{in} and, f is antenna impedance, antenna resistance, antenna reactance and frequency respectively. In general, antenna resistance consists of two components as shown in equation (2.17).

$$R_{in} = R_r + R_l \quad (2.17)$$

where R_r and, R_l is radiation resistance of the antenna and, loss resistance of the antenna. The antenna has an equivalent circuit can be represented in figure (2.9). The equivalent circuit of antenna is connected to the generator that has internal impedance $Z_s = R_s + jX_s$ and the antenna has impedance $Z_{in} = R_a + jX_a$ [9].

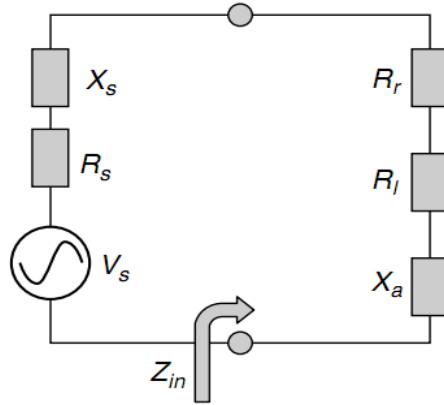


Figure (2.9): Equivalent circuit of antenna [9]

Input impedance is important parameter. We can determined different parameter from it like reflection coefficient (Γ), Return Loss (RL) and, voltage standing wave ratio (VSWR) as a function of frequency as given in equation (2.18)

$$\Gamma = \frac{Z_{in} - Z_o}{Z_{in} + Z_o} \quad (2.18)$$

where Z_o is the normalized impedance of the port, but if its complex the reflection coefficient become

$$\Gamma = \frac{Z_{in} - Z_o^*}{Z_{in} + Z_o} \quad (2.19)$$

where Z_o^* is the conjugate of nominal impedance. The VSWR is give as

$$VSWR = \frac{1 + |\Gamma|}{1 - |\Gamma|} \quad (2.20)$$

and the return loss is defined as

$$RL = -20 \log \Gamma \quad (2.21)$$

2.6 Microstrip Patch Antenna

RF and microwave technology are rapidly finding their way to commercial and consumer products. These technologies are basically used for specially design communication system. Engineers often find themselves in a position that needs to improve this technology to serve in various areas such as antenna and RF circuit[8]. Microstrip antennas (also known as patch antennas) are used widely in the wireless communication system due to its simplicity and compatibility with printed circuit technology. In most applications that need a high performance like missiles, spacecraft, air craft, satellite, a small size, good performance, and ease of installation antenna is needed. To meet these requirements a microstrip antenna can be used. It provides high data rate transmission which allows the industry to provide greater quality of services to the end users. Like any technology we know, there are advantages and disadvantages of these antenna that can be summarized in a few points [7].

Advantages of microstrip antenna

1. Light weight and low volume.
2. Low profile and planar configuration.
3. Low fabrication cost, hence it can be manufactured in large quantities.
4. Can be easily integrated with microwave integrated circuits (MICs).
5. Capable of dual and triple frequency operations.

Disadvantages of microstrip antenna

1. Narrow bandwidth
2. Low efficiency
3. Low Gain
4. Low power handling capacity [11].

The origin of microstrip antennas was conceived in 1953, when Deschamps proposed the use of microstrip feed lines to feed an array of printed antenna elements. Then the first was introduced by Munson in 1972, 1974 when he discussed both the microstrip antenna and the rectangular patch [7]. After decades of research, it was found that the performance and operation of a

microstrip antenna is dependent on the geometry of the printed patch and the material characteristics of the substrate onto which the antenna is printed[6].

2.6.1 Basic Characteristics

Microstrip antenna simplicity consist, as shown in figure (2.9) of a pair of parallel conducting elements separated by a dielectric medium, referred to as substrate. The upper element is the radiator called patch where electromagnetic energy fringes off the edges of the patch and into the substrate, and the lower is the ground plane which is perfectly a reflection, that reflects the electromagnetic energy back through the substrate and into free space [11].

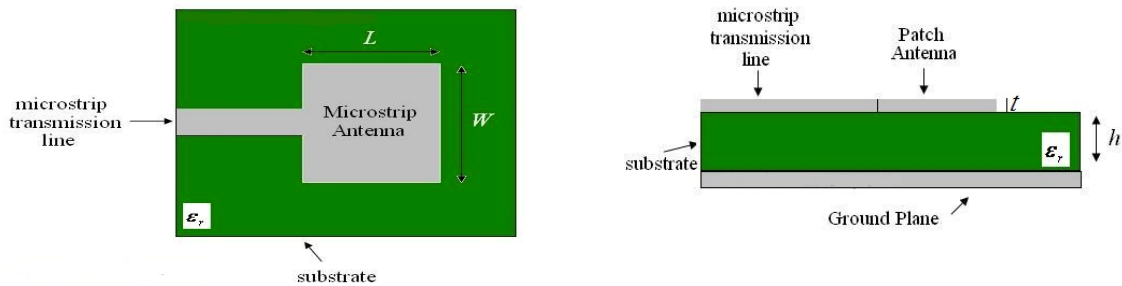


Figure (2.9-a): Top view of patch antenna[12] (b) Side view of patch antenna[12]

The electric field is zero at the center of patch and its maximum (positive) at one side and minimum (negative) at the opposite side as show in figure (2.10). It should be known that the maximum and minimum is changeable according to the exited signal phase that applies to the patch. This field is extended outside around the patch to some degree. This field is called fringing field which causes the radiation of the patch [13].

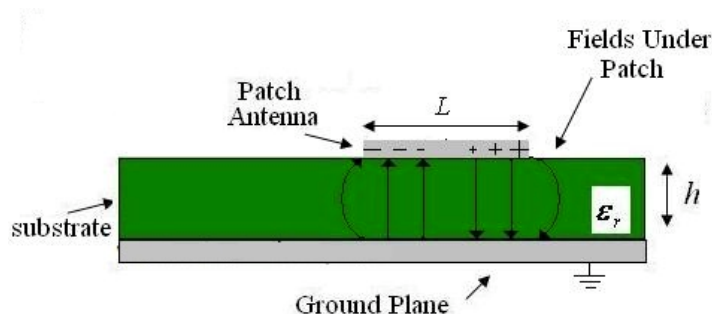


Figure (2.10): Electric field distribution on patch antenna[12]

The patch has a very small thickness ($t \ll \lambda_0$) which λ_0 denotes to wave length in free space . The substrate high which is the distance that separates ground plane from patch is also small ($h \ll \lambda_0$ usually $0.003\lambda_0 \leq h \leq 0.05\lambda_0$). There are different types of the dielectric material that is used in substrate with different dielectric constant. It's usually placed in range $2.2 \leq \epsilon_r \leq 12$. The radiation of the patch antenna largely depends on the permittivity ϵ_r of the dielectric material. For a good antenna performance a thick substrate with a small dielectric constant are used because they provide better efficiency, larger bandwidth, loosely bound fields for radiation into space, but the size of antenna well be large. Thin substrates with higher dielectric constants lead to smaller element sizes and minimize undesired radiation, however, because of their greater losses, they are less efficient and have relatively smaller bandwidths. For rectangular patch the length of it L is usually choose in range $\lambda_0 / 3 \leq L \leq \lambda_0 / 2$. The patch may have a different shape. As show in figure (2.11) bellow it may be square, rectangular, thin strip (dipole), circular, elliptical, triangular, or any other configuration. Square, rectangular, and circular are the most commonly used because of ease of analysis and fabrication, and their attractive radiation characteristics [6].

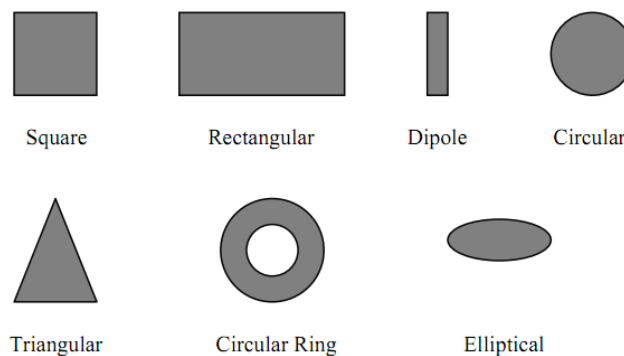


Figure (2.11): Common shapes of microstrip patch elements[6]

2.6.2 Feeding Techniques

There are different techniques using for exiting the patch antenna. There are some factors must be achieved in using feeding technique such as effective transfer power between radiating structure and feed structure, impedance matching between radiating structure and feed structure, reducing the effect of undesired radiation on radiation pattern (Sid lob), suitable of the feed in

array application. Microstrip patch antennas can be fed by using variety methods. These methods can be classified into two categories. Feeding by direct contact like (Microstrip feed line & Coaxial probe feed) and, feeding by non-direct contact (coupling) like (Aperture-Coupled antenna& Electromagnetically Coupled ECMSA). These feeding methods could be consider as the most popular four feed techniques are used [14].

2.6.2.1 Microstrip Feed Line

In this type of feeding a microstrip transmission line is etched directly to the edge of patch which remain the total structure in same planer as shown in figure (2.11), so the patch can be considered as extension of microstrip line and can be fabricated simultaneously. The width of microstrip line is small compared to patch. Input impedance is easily controlled using the matching stub. This stub achieved impedance matching without the need for any additional matching elements [11].

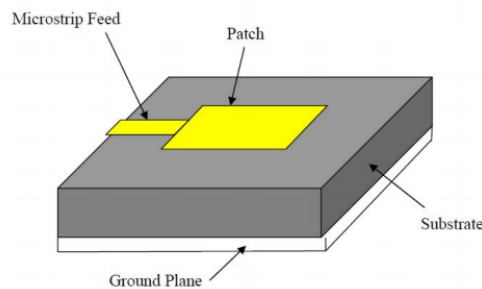


Figure (2.12): Microstrip feed line[24]

2.6.2.2 Coaxial Feed /Probe Coupling

The coaxial or probe feed is shown in figure (2.13). The inner conductor of coaxial connector is passing through the substrate and is soldered to the radiating patch, while the outer conductor is connected to the ground plane. The main advantage of this feed is that the connector can be placed at any direction location inside the patch to achieve matching impedance. But the hole caused by drilling the substrate to pass the connector and that the connector protrudes outside the bottom ground plane cause the total structure to be not completely planner. There are some limitations in using these methods in feeding, like that in array application a large number of joints is required which makes fabrication difficult.

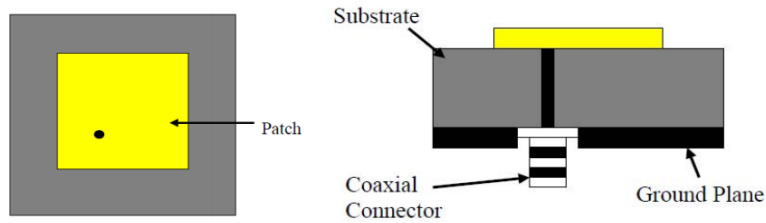


Figure (2.13): Coaxial cable feed of patch antenna [24]

For thick substrates, which are generally employed to achieve large bandwidth, both the above methods of direct feeding the MSA have problems. For the microstrip feed line, an increase in the substrate thickness cause an increases in the microstrip feed width, which increase the undesired feed radiation. Also the drawback of increase the substrate thickness in the case of a coaxial feed is that increased probe length makes the input impedance more inductive, leading to the matching problems [11]. These problems can be solved by using indirect feeding methods.

2.6.2.3 Aperture-Coupled Feed

In this type of feed the aperture coupling consists of two substrates separated by a ground plane. The ground plane is separated the radiating patch and microstrip line which locate at the bottom of lower substrate. The coupling is achieved through an electrically small aperture or slot cut in the ground plane, as shown in figure (2.14). The amount of coupling between patch and microstrip line is determined by the size, shape, and the location of aperture [11]. For a bottom substrate a high dielectric material is used and thick. Lower dielectric material can be used for atop substrate to optimize radiation from the patch. The matching can be controlled by optimized the width of feed line and the length of slot [6]. The major disadvantage of this feed technique is that difficult to fabricate due to multiple layers, which also increases the antenna thickness [14].

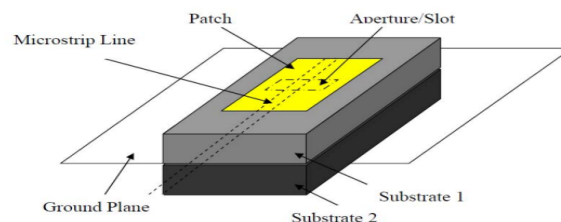


Figure (2.14): Aperture coupled feed [14]

2.6.2.4 Proximity-Coupled Feed

It's also called Electromagnetically Coupled ECMSA. It's also consisting of two substrates. The microstrip feed line is located between two substrates and the radiating patch is located on the top of the upper substrate as shown in figure (2.15). Of the four feeds described here, the proximity coupling has the largest bandwidth (as high as 13 percent), due to the overall increase in the thickness of the microstrip patch antenna. It's also easy to model and has low spurious radiation. The choice of two different dielectric media, one for the patch and one for the feed line, can optimize the individual performances. The major disadvantage of this feed scheme is that it is difficult to fabricate because of the two dielectric layers which need proper alignment. Also, there is an increase in the overall thickness of the antenna [14].

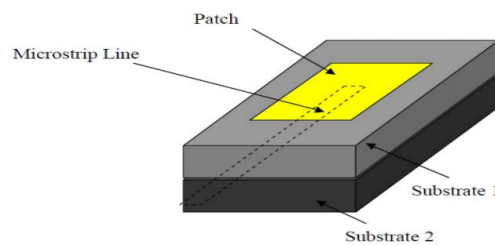


Figure (2.15): Proximity coupled feed[14]

2.7 Microstrip Transmission Line

Transmission line structures are techniques that provide guided waves over limited distances that are compatible with circuit construction. It's a planar form of a single wire transmission line placed over a ground plane, called microstrip. Microstrip employs a flat strip structure suspended above a ground plane and separated by a dielectric medium as shown in figure (2.16)[9].

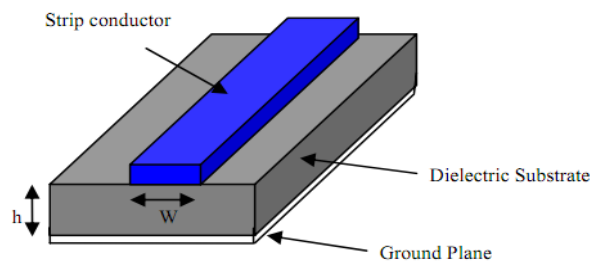


Figure (2.16): Microstrip line[14]

The dielectric material serves as a substrate and it is sandwiched between the strip conductor and the ground plane. Important physical parameters of the microstrip line include the line width, w , substrate height, h , strip conductor thickness, t , and substrate relative dielectric constant, ϵ_r . Important electrical parameters for microstrip line design are the characteristic impedance, Z_0 and, the guide wavelength, λ_g [7]. The electromagnetic wave on the transmission line will lie somewhere between the air and dielectric as shown in figure (2.17).

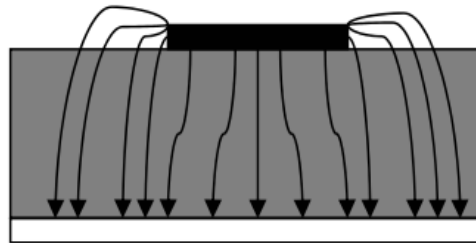


Figure (2.17): Electric field line [12]

The phase velocity of electromagnetic wave on the microstrip line will be determined by using the effective dielectric constant. The effective relative dielectric constant ϵ_{eff} is a very important concept in design microstrip line. The most challenging problems that faced the designer is that the small strip is not immersed in a single dielectric. On one side there is dielectric, and on the top is usually air. The techniques that are used to overcome this challenge is the concept of effective relative dielectric constant ϵ_{eff} . This value represents some intermediate value between the relative dielectric constant of material, ϵ_r , and that of air (assumed equal to 1). It can be used to compute microstrip parameters and, the strip will be assumed as completely surrounded by material of that effective relative dielectric constant. Effective relative dielectric constant will depend on both the width of microstrip line w and in the high of substrate h , also the phase velocity along the microstrip line will depend on this parameter. The guide phase velocity v_g is given by equation (2.22)

$$v_g = \frac{c}{\sqrt{\epsilon_{eff}}} \quad (2.22)$$

where c is the speed of light = $3 \times 10^8 \text{ m/s}$. Relative permeability of all materials in the line

design will be approximated by $\mu_r = 1$ the guide wavelength, λ_g are given by equation (2.23).

$$\lambda_g = \frac{v_g}{f} = \frac{c}{f\sqrt{\epsilon_{eff}}} = \frac{\lambda_0}{\sqrt{\epsilon_{eff}}} \quad (2.23)$$

Form the above equation we note that the characteristic impedance Z_0 of microstrip line will also depend on this parameters, (w, h) , so every time we need to design a microstrip with a new characteristic impedance, we will be faced with the additional complication of new phase velocity (or delay time) and consequently of the wavelength of waves on that microstrip. We can handle this problem by assuming two causes to get an idea range of ϵ_{eff} . The first, assuming that the microstrip line is very wide and the second is that it is very narrow. In first cause the electric field lines will be concentrated between the metal planes given by equation (2.24)

$$\max \epsilon_{eff} = \epsilon_r \quad (2.24)$$

In the second case the electric field lines will be about equally divided between the air and the board dielectric and given by equation (2.25)

$$\min \epsilon_{eff} = 0.5(\epsilon_r + 1) \quad (2.25)$$

So the range become as shown in equation (2.26),

$$0.5(\epsilon_r + 1) \leq \epsilon_{eff} \leq \epsilon_r \quad (2.26)$$

The characteristic impedance Z_0 can be calculated using straightforward equations that have been developed for design given w, h, ϵ_{eff} as shown in equations (2.27-2.30),

for $\frac{w}{h} \geq 1$

$$\epsilon_{eff} = \frac{(\epsilon_r + 1)}{2} + \frac{(\epsilon_r - 1)}{2} \left[1 + 12 \frac{h}{w} \right]^{-1/2} \quad (2.27)$$

$$Z_0 = \frac{120\pi}{\sqrt{\epsilon_{eff}} \left[\frac{w}{h} + 1.393 + 0.667 \ln \left(\frac{w}{h} + 1.444 \right) \right]} \quad (2.28)$$

for $\frac{w}{h} \leq 1$

$$\varepsilon_{eff} = \frac{(\varepsilon_r + 1)}{2} + \frac{(\varepsilon_r - 1)}{2} \left[\left(1 + 12 \frac{h}{w} \right)^{-0.5} + 0.04 \left(1 - \frac{w}{h} \right)^2 \right] \quad (2.29)$$

$$Z_0 = \frac{60}{\sqrt{\varepsilon_{eff}}} \ln \left(8 \frac{h}{w} + \frac{w}{4h} \right) \quad (2.30)$$

To make things a bit more challenging, we'll introduce a further "correction" to the above equations which considers the finite thickness t of the microstrip line. This correction is in the form of an "effective" microstrip width w_{eff} , which is replaced with w in those equations as shown in (2.31-3.32),[15].

for $\frac{w}{h} \geq 1$

$$w_{eff} = w + \frac{t}{\pi} \left[1 + \ln \left(\frac{2h}{t} \right) \right] \quad (2.31)$$

for $\frac{w}{h} \leq 1$

$$w_{eff} = w + \frac{t}{\pi} \left[1 + \ln \left(\frac{4\pi w}{t} \right) \right] \quad (2.32)$$

2.8 Microstrip Transmission Line Matching

The input impedance of patch antennas depends on their geometrical shape, dimensions, the physical properties of the materials involved, the feed type and location. Therefore, a subset of antenna parameters can be adjusted to achieve the best geometry for matching. There is different method to controlling impedance match for microstrip line with patch antenna like, Inset Feed, and Quarter-Wave Transformer [16] .

2.8.1 Inset Feed

One of the matching techniques is using inset feed as shown in figure (2.18). Since the current is low at the edge of patch whose length L is half-wavelength and increase in magnitude toward

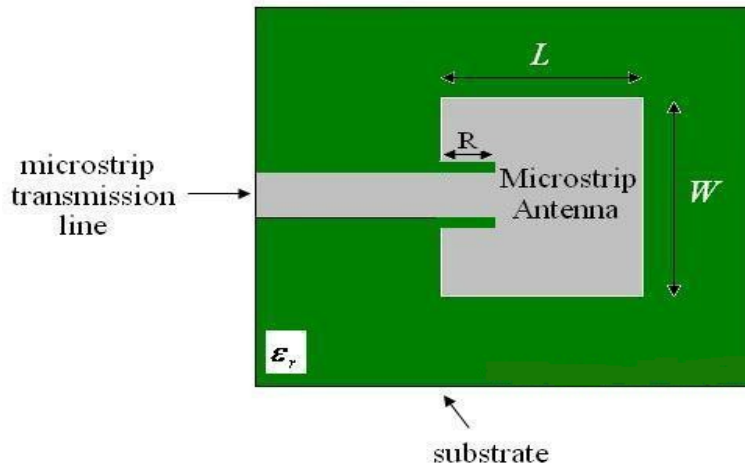


Figure (2.18): Patch antenna with an inset feed[12].

the center, the input impedance $Z_{in} = \frac{V}{I}$ could be very large if the patch feeds from the edge and very small if the patch feeds from the center. So, to control input impedance, matching inset feed (distance R from edge) have been used.

The experimental and numerical results showed that a shifted \cos^2 function work well for inset feed. Since the current distributed sinusoidal moving from the edge toward the center will increase by $\cos\left(\frac{\pi R}{L}\right)$ -since the wavelength is $2L$ so the phase different $=\left(\frac{2\pi R}{2L}\right)=\left(\frac{\pi R}{L}\right)$ - also the voltage is decreased as the same amount of the current increases. The input impedance scales given is as shown in equation (2.33),[12]

$$Z_{in}(R) = \cos^2\left(\frac{\pi R}{L}\right) Z_{in}(0) \quad (2.33)$$

where $Z_{in}(0)$ is the input impedance when the patch feeds from the edge and, it can be found for rectangular patch form equation (2.34-2.37) below:

$$W_p = \frac{v_o}{2f} \sqrt{\frac{2}{\epsilon_r + 1}} \quad (2.34)$$

$$G_1 = \frac{1}{120\pi^2} \int_0^\pi \left[\frac{\sin\left(\frac{K_0 W_p}{2} \cos\theta\right)}{\cos\theta} \right]^2 \sin^3\theta d\theta \quad (2.35)$$

$$G_{12} = \frac{1}{120\pi^2} \int_0^\pi \left[\frac{\sin\left(\frac{K_0 W_p}{2} \cos\theta\right)}{\cos\theta} \right]^2 j_0(K_0 L_p \sin\theta) \sin^3\theta d\theta \quad (2.36)$$

$$Z_{in} = \frac{1}{2(G_1 + G_{12})} \quad (2.37)$$

where $K_0 = \frac{2\pi}{\lambda}$ is free space wave number and j_0 is the Bessel function of the first kind of order zero and, W_p patch width[17].

2.8.2 Quarter-Wave Transformer

Figure (2.19) shows the Quarter-Wavelength Transformer. Recall to formula for the input impedance of a transmission line of length L with characteristic impedance Z_0 and connected to a load with impedance Z_A given by equation (2.37).

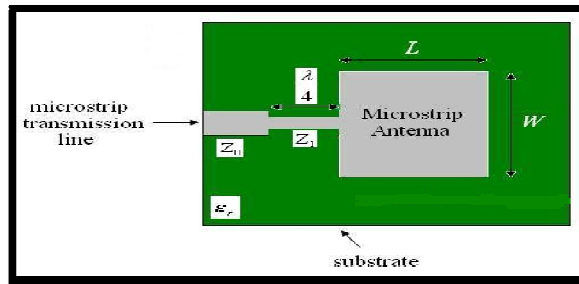


Figure (2.19): Patch antenna with a quarter-wavelength matching section[12]

$$Z_{in}(L) = Z_0 \left[\frac{Z_A + jZ_0 \tan(\beta L)}{Z_0 + jZ_A \tan(\beta L)} \right] \quad (2.37)$$

where $\beta = \frac{2\pi}{\lambda}$, λ is wavelength number ,and wavelength respectively. If the length of transmission line is a quarter of a wavelength there is an interesting thing that happens. The above equation becomes like

$$Z_{in}(L = \frac{\lambda}{4}) = Z_0 \left[\frac{Z_A + jZ_0 \tan(\frac{2\pi}{\lambda} \frac{\lambda}{4})}{Z_0 + jZ_A \tan(\frac{2\pi}{\lambda} \frac{\lambda}{4})} \right] \quad (2.38)$$

so the result is :

$$Z_{in}(L = \frac{\lambda}{4}) = \frac{Z_0^2}{Z_A} \quad (2.39)$$

The above equation is important. It states that the lode with characteristic impedance can be transformed using the above equation if the Quarter-Wavelength is used for transmission line length[18].

Chapter 3

UWB Antennas and Finite Element Method

3.1 UWB Antennas Characteristic

Designing UWB antennas is the main challenge in wireless communication system. For any wireless system there are four typical requirements that may be handled by antenna either for narrowband or ultra-wideband. One of them achieved high efficiency, ability to detect signal at receiver, also the ability to specify radiation pattern depending on application and, finally acceptable radiated power in free spaced that complies with regulator's limits.

Antenna gain, impedance matching, and polarization are traditional parameters that are enough to assess the antenna performance in narrowband system but, if we talk about UWB antenna there is additional parameter that we must take into account to get good performance. Efficiency is important parameter especially for portable device like laptop and, mobile whose power supply is limited. For UWB system radiation efficiency is obtain using equation (3.1)

$$\eta_{(uwb)} = \frac{\int_0^{\infty} P_{exc}(f)(1-|S_{11}(f)|^2)df}{\int_0^{\infty} P_{exc}(f)df} \quad (3.1)$$

which $P_{exc}(f)$,and $|S_{11}(f)|$ is exciting power and return loss respectively and, both of them are frequency dependent. Form equation (3.1) above we can see that the radiation efficiency is dependent on spectrum of a source and not only on the antenna parameter $|S_{11}(f)|$.

To increase the system's efficiency, good impedance matching over the band of a source is expected. In narrow band system the radiation efficiency is obtain from equation (3.2)

$$\eta_{(nb)} = 1 - |S_{11}|^2 \quad (3.2)$$

The scheme of signal detection in UWB systems at receiver is different from that in narrowband systems. In narrowband system the received signal can be detected easy in Additive White Gaussian Noise (AWGN) channel if the signal to noise ratio is high. Using local oscillator (LO) can help to detect received signals in narrowband systems because there is a carrier. In contrast, there is no carrier in UWB systems which makes the signal detection operate in a different way. Another important parameter for the antenna design is radiation pattern. In narrowband system the modulated signal can be detected successfully with enough radiated power along desired directions. In UWB system high radiated power along desired directions is not enough for detecting signal successfully [19]. However, there are more challenges in designing a UWB antenna than a narrow-band one. First of these challenges is, according to FCC definition, the UWB antenna should be able to yield bandwidth no less than 500MHz. Secondly, the performance of antenna is required to be constant over the entire operational band. Radiation patterns, gains and impedance matching should be stable across the entire band. Thirdly, depending on the practical application directional or Omni-directional radiation properties are needed. Lastly, but not the least important, the size of antenna must be suitable and compatible for devices like that in portables devices such as mobile, laptop, iPad and wireless access point the antenna should be small size[3].

3.2 Types of UWB Antenna

There are different types of UWB antenna depending on radiating characteristic: travelling wave, frequency independent antennas, small element antennas and, multi-resonant antennas [20].

3.2.1 Travelling Wave Antennas

Figures (3.1) and (3.2) below show horn antenna and, tapered slot antennas which is classified as travelling wave antennas. It is considered as gradual transition between a guided wave and a radiated wave. It has good UWB properties. Horn antenna can be considered as major class of UWB directional antenna and it is mainly used for ground radar application. It is consisting of

rectangular or circular waveguides which are naturally broadband. Their bandwidth is relatively large.

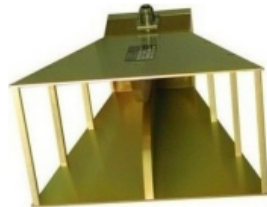


Figure (3.1):Horn antenna [20]

The tapered slot antenna is also class of UWB directional antenna. It consists of a tapered slot that has been etched on metallization placed above substrate. The tapering has different form: linear tapered slot antenna (LTSA), constant width slot antenna (CWSA), broken linearly tapered slot antenna (BLTSA) or exponentially tapered slot antenna (Vivaldi) as shown in figure (3.2) below. Their bandwidth is relatively large [20].

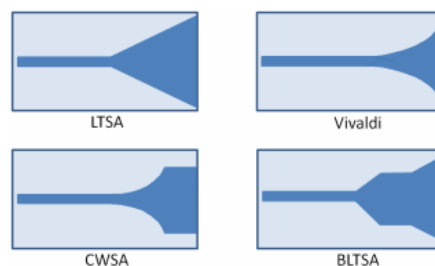


Figure (3.2): LTSA, Vivaldi, CWSA and, BLTSA[20]

3.2.2 Frequency Independent Antennas

Logarithmic spiral, spiral, conical spiral and log periodic antennas shown in figure (3.3) below are frequency independent antennas and classified as broadband and UWB antennas. These parameters such as impedance and radiation patterns are constant over a frequency bandwidth greater than 10:1. There are two principles to achieve frequency independence. First, if the antenna shape is specified only in terms of angle without specifying any characteristic length dimensions then the antenna can be considered frequency independent. Infinite logarithmic spiral and spiral

antennas are good examples for that, the shape of both antennas are completely specified in terms of angle. But in loge periodic antenna the shape is depend on the length from the origin to any point on the structure and it still exhibits frequency independent characteristics. The second principle for frequency independent characteristics is self complementarities which state that the input impedance is constant and, independent of the source frequency and of the shape of the structure [21]. Hence if the antenna is its own complement the frequency independent impedance behavior is obtained. The frequency independent antennas can operate over an extremely wide frequency range [20].

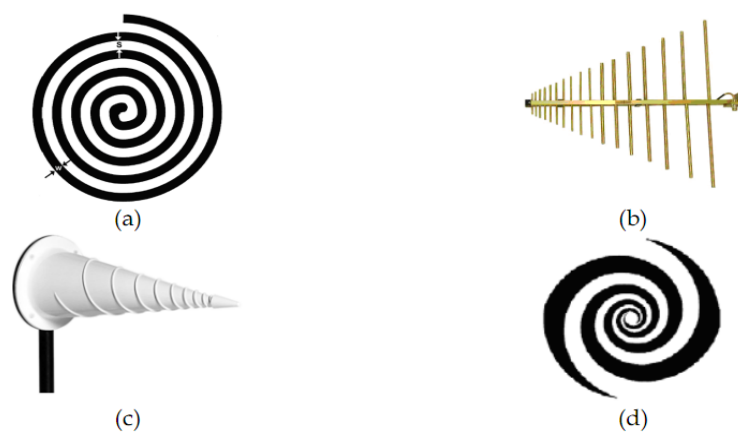


Figure (3.3): spiral, log periodic, conical spiral and logarithmic spiral antennas [20]

3.2.3 Small Element Antennas

Small-element antennas as Lodge’s biconical and bow-tie antennas, Mater’s diamond dipole, Stohr’s spherical and ellipsoidal antennas, and Thomas’s circular dipole have been shown in figure (3.4) below. These antennas come from direct development of dipole and monopole antennas. Antenna engineers found that thickening the arms of dipole and monopole antennas cause increase in the bandwidth. This results from the fact that the current distribution is no longer sinusoidal, which has little effects on radiation patterns of the antenna and stronger effect on the input impedance. figure (3.4, a-b) shows the evolution of thin-wire dipole antenna towards a biconical antenna. The band widening is affected more if the thick dipole takes the shape of a biconical antenna which also presents a frequency independent impedance response. Figure (3.4,c) presented a single core antenna and figure (3.4,d-e) presented alternative possible asymmetrical structures. The bow-tie antenna which is a flat version of biconical antenna

presented in figure (3.4,f) and the replacement of one pole by ground plane is presented in figure (3.4,g-h).

Monopole antennas are widely used in wireless communication system due to simple structure, low cost and easy matching with 50Ω . The bandwidth of straight wire monopole is typically around 10% - 20%.

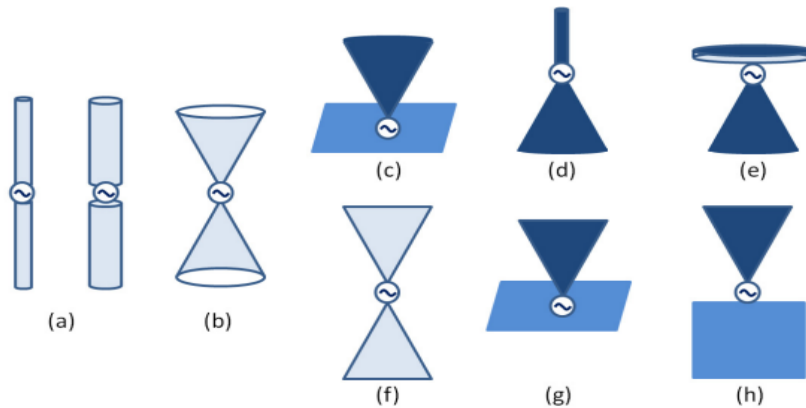


Figure (3.4): Monopole, biconical, single core, and, bow-tie antennas[20]

The bandwidth of monopole is dependent on the ration between radius and length of monopole. If the radius of monopole is large compared with the feed line the impedance mismatch is cured and the bandwidth not increase. To increase the bandwidth the thin wire are replaced by a plate. This plate may take different shapes triangle, circular, square, trapezoid, pentagonal, hexagonal, elliptical as shown in figure (3.5) [20].

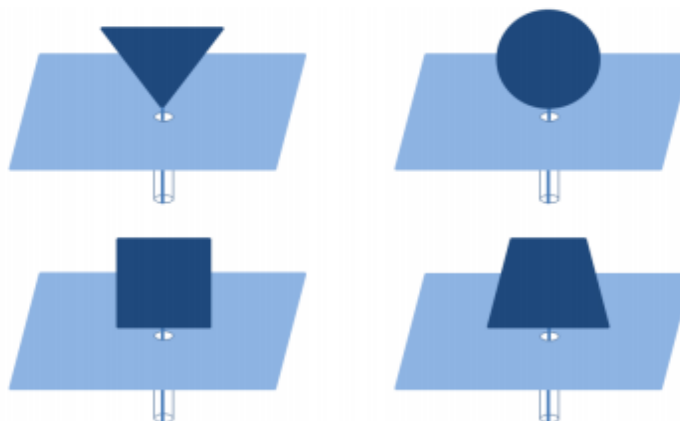


Figure (3.5): Different plate shape[20]

3.2.4 Multi-Resonant Antennas

Multi resonant antennas are composed of a multiple of narrowband of radiating elements like log periodic antennas or Yagi antennas. This antenna is classed as UWB antenna. It is not convenient for UWB systems because its phase centers are not fixed in frequency [20].

3.3 Numerical Solution

There are several techniques used to solve field problems. These techniques can be classified in to, experimental, analytical, and numerical method. Experimental methods could be expensive, time-consuming and hard to apply because of a shortage of some of the requirement. Numerical methods such as Finite Element Method (FEM), Moment Method (MoM) and Finite Difference Method (FDM) which have given approximated solutions may be easier than analytical methods which given exact solutions because it involves an analytic simplification to the problems. In the mid-1960s a Numerical solution of EM problems was started with the availability of modern high-speed digital computers. The advantage of numerical solution is allowing the actual work to be carried out without need to know of higher mathematics or physics [22]. Before we start to study these techniques we need to review the electromagnetic theory.

3.3.1 Review of Electromagnetic Theory

Studding EM fields starts from the electric charge. Field produced form electric charge whether this charge is in rest or in motion. Electrostatic field is produced when the electric charge is in rest and, the magnetostatic field is produced if the electric charge is in motion with uniform velocity. Dynamic or time varying field occurs when the charges are accelerate or the current changing with time [22]. The general theory of electromagnetic phenomena is based on Maxwell's equations. Its constitutes a set of four coupled first-order vector partial-differential equations relating to the space and time changes of electric and magnetic fields to their scalar source densities (divergence) and vector source densities (curl)[23].

For Time-varying Fields, both electric and magnetic fields exist simultaneously. Maxwell's equations are usually formulated in two forms, differential form or in integral form. Differential form of Maxwell's equations are given by equation (3.3-3.6):

$$\nabla \cdot D = \rho_v \text{ (Gauss law)} \quad (3.3)$$

$$\nabla \cdot B = 0 \text{ (Gauss law for magnetic fields)} \quad (3.4)$$

$$\nabla \times E = -\frac{\partial B}{\partial t} - J_m \text{ (Faraday s law)} \quad (3.5)$$

$$\nabla \times H = J_e + \frac{\partial D}{\partial t} \text{ (Generalized Ampère s law)} \quad (3.6)$$

Integral form of Maxwell's equations (3.7-3.10):

$$\oint_s D \cdot ds = \int_v \rho_v dv \text{ (Gauss law)} \quad (3.7)$$

$$\oint_s B \cdot ds = 0 \text{ (Gauss law for magnetic fields)} \quad (3.8)$$

$$\oint_L E \cdot dl = -\int_s \left(\frac{\partial B}{\partial t} + J_m \right) \cdot ds \text{ (Faraday s law)} \quad (3.9)$$

$$\oint_L H \cdot dl = \int_s \left(J_e + \frac{\partial D}{\partial t} \right) \cdot ds \text{ (Generalized Ampère s law)} \quad (3.10)$$

where D is electric flux density (in coulombs/ meter²), ρ_v is the volume charge density (in coulombs/meter³), H is the magnetic field intensity (in amperes/meter), E is the electric field intensity (in Newton/coulombs), J_e electric current density (in amperes/meter²), B magnetic flux density (in tesla or webers/meter²) and, J_m is the magnetic conductive current density (in volts/square meter) [23]. In addition to these four Maxwell's equations, there are four medium-dependent equations given by equation (2.11-2.14) which are called constitutive relations for the media in which the field exist. where ϵ is the dielectric permittivity (in farads/meter) of the

$$D = \epsilon E \quad (3.11)$$

$$B = \mu H \quad (3.12)$$

$$J_e = \sigma E \quad (3.13)$$

$$J_m = \sigma * M \quad (3.14)$$

medium, μ is the permeability (in henries/meter) , σ is the conductivity (in mhos/meter) of the medium , and σ^* is the magnetic resistivity (in ohms/meter)of the medium[23].

3.3.2 Finite Element Method (FEM)

Finite element method is a strong and stable numerical technique that can analyses a complex problem to give out approximate solutions. It was introduced by Turner et al. (1956) as a powerful computational technique. The basis of FEM is decomposing the domain into finite number of subdomains (element) without leaving any gaps or allowing any overlapping between them[24]. There are lots of shapes the elements can have. From segments of lines, triangles and squares specifically, FEM discretizes the problem domain using triangular elements.

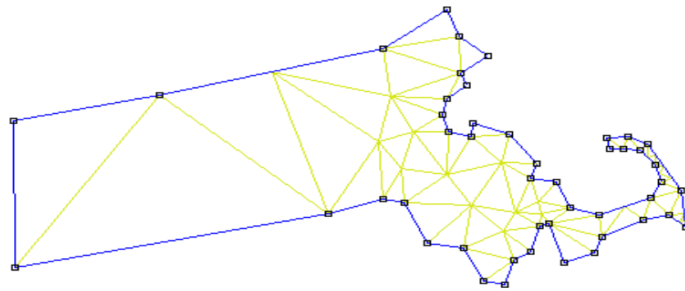


Figure (3.6): Division of irregular domain in to triangular[25]

One of the advantages of divided the domain in to triangular elements is that irregular regions can be more easily approximately covered by a set of triangular as shown in the Figure (3.6)[25].

3.3.2.1 Solving Differential Equation using FEM for One Dimension

In one dimensional problem the solution of differential equation using FEM based on dividing the region into finite numbers of segments as shown in example below. Consider the ordinary differential equation

$$\frac{d^2u}{dx^2} = f(x) \text{ in } (0, L), \quad (3.15)$$

$$u(0) = u_0, \quad (3.16)$$

$$u(L) = u_L, \quad (3.17)$$

Let N point chosen in the interior of the domain $(0, L)$ each of them equidistance from its immediate neighbor as shown in figure (3.7) below:

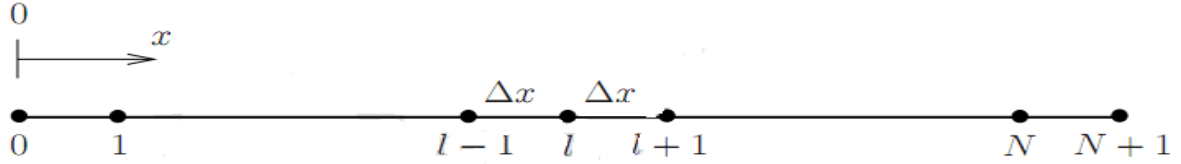


Figure (3.7): The Finite element method for one dimensional[8]

Now consider the line segment between point l and $l+1$. This is now the domain of the finite element e . In this domain we assume that u is various lineally as shown in figure (3.8):

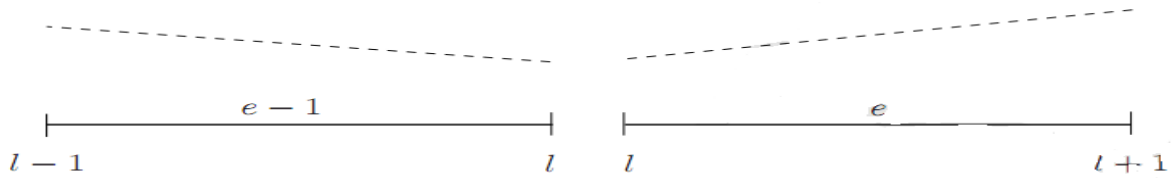


Figure (3.8): One-dimensional FEM approximation[8]

and attains a value at point l is u_l and at point $l+1$ is u_{l+1} . Assume that the differential function at the domain of the finite element e at both point l and $l+1$ is given by q_l^e and q_{l+1}^e , where,

$$q_l^e = \frac{u_{l+1} - u_l}{\Delta x} \quad (3.18)$$

$$q_{l+1}^e = \frac{u_l - u_{l+1}}{\Delta x} \quad (3.19)$$

the above equation can be written in matrix form as

$$\frac{-1}{\Delta x} \begin{bmatrix} 1 & -1 \\ -1 & 1 \end{bmatrix} \begin{bmatrix} u_l \\ u_{l+1} \end{bmatrix} = \begin{bmatrix} q_l^e \\ q_{l+1}^e \end{bmatrix} \quad (3.20)$$

Also it can be written for element e_{l-1} , whose domain lies between point $l-1$ and l

$$\frac{-1}{\Delta x} \begin{bmatrix} 1 & -1 \\ -1 & 1 \end{bmatrix} \begin{bmatrix} u_{l-1} \\ u_l \end{bmatrix} = \begin{bmatrix} q_{l-1}^{e-1} \\ q_l^{e-1} \end{bmatrix} \quad (3.21)$$

Now by adding equation (3.20) to (3.21) it yields to

$$\frac{1}{\Delta x} (u_{l+1} - 2u_l + u_{l-1}) = q_l^e + q_l^{e-1} \quad (3.21)$$

At the same time one may rewrite the differential equation as $\frac{du}{dx} = \int f(x).dx$. Hence, if the $f(x)_{total} = \int_L^0 f(x).dx$ is distributed to the point $0, 1, \dots, N+1$ so to the point l corresponds to

$$\tilde{f}_l(x) = \frac{1}{\Delta x} (u_{l+1} - 2u_l + u_{l-1}) \quad (3.22)$$

Then, the complete finite element system become, [8]

$$u_2 - 2u_1 = \tilde{f}_1(x) \Delta x - u_0 \quad (3.23)$$

$$u_{l+1} - 2u_l + u_{l-1} = \tilde{f}_l(x) \Delta x - u_0 \quad L = 2, \dots, N-1 \quad (3.24)$$

$$-2u_N + u_{N-1} = \tilde{f}_N(x) \Delta x - u_L \quad (3.25)$$

3.4 Literature Review and Methodology

Many UWB antennas have been studied and discussed in the literature in order to achieve the requirement for different applications. Gain enhancements and bandwidth expansions are the most important requirements. Since microstrip patch antennas inherently have narrow bandwidth characteristics, there have been numerous techniques developed for bandwidth enhancement in order to achieve the UWB characteristics.

K.-S. Lim, [26] proposed a compact Ultra Wide Band (UWB) microstrip antenna. The proposed antenna has the capability of operating between 4.1 GHz to 10 GHz. But his antennas have bandwidth narrower compared with the bandwidth allocated by FCC which is from 3.1 GHz to 10.6 GHz. One of the techniques that used to enhance the bandwidth of antenna is found in [27]. They proposed that the antenna consists of a rectangular patch with two steps, single slot on the patch and, a partial ground plane as shown in figure (3.9). The antenna operates from 3.2 to 12 GHz is better than that found in [26] since it has a wider bandwidth and a more stable gain in bandwidth range.

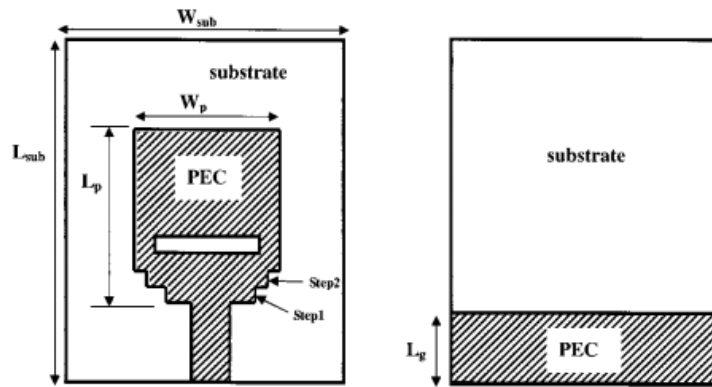


Figure (3.9): Patch with single slot and partial ground plane [27].

Another technique that has given good results and shown less complexity in structure depends on a small cut on the outskirts of patch as shown in figure (3.10) is found in [28]. A new planar monopole ultra-wideband (UWB) antenna was proposed. It consists of an octagonal shape patch with a transmission line edge feed and an underlying ground plane, an antenna that achieves an ultra-wide bandwidth starting from 2.23716 GHz and ending at 15.4495 GHz.



Figure (3.10): Antenna with small cut on the outskirts of patch[28].

Recently other techniques have been examined to enhance the bandwidth of UWB antenna including the insertion of a modified shape of a short ground plane which is also having compact profile and suitable to be integrated with PCB. Tariqual et al [29] introduced a microstrip printed rectangular antenna structure which consists of a square patch and a partial ground plane with a multiple rectangular slot at top side as shown in figure (3.11), the result shows that the antenna

achieves impedance bandwidth from 2.77 to 17.62GHz, the drawback of these designs is the low gain, the gain variations are less than about 1.5 dBi in bandwidth range.

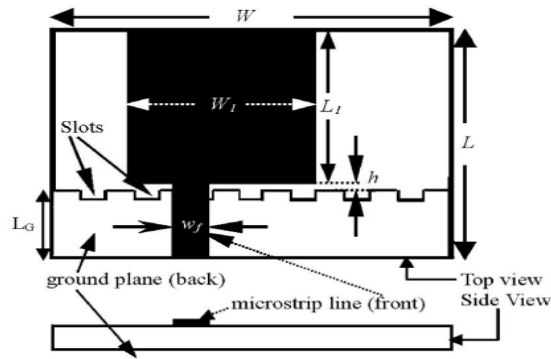


Figure (3.11): Antenna with partial ground plane with multiple rectangular slot at top side[29].

Techniques such as adding step to the lower edge of patch at both sides with horizontal slot on patch have been studied on [27], the same techniques used with slight differences were found in [30]. The proposed antenna exhibits excellent performance of UWB characteristics with enhanced bandwidth, with impedance bandwidth from 3.34 GHz to 20 GHz, The antenna consists of a larger patch with an etched slot at the lower edge of antenna with a vertical slot on the patch and a small cut on the ground plane as shown in figure (3.12).

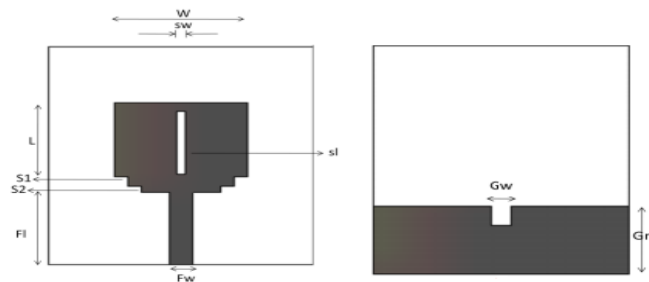


Figure (3.12): Antenna with an etched slot at the lower edge and vertical slot on the patch and a small cut on the ground [30].

Another technique to broaden the impedance bandwidth of small antennas are found in [31]. A rectangular planar antenna has the operating bandwidth ranging from 3GHz-8GHz by integrating various technologies into one. By truncated ground plane, and adding extra patch printed on the back side of the substrate, underneath the rectangular radiator as shown in figure (3.13) the

bandwidth can be further increased to cover wide bandwidth. The disadvantage of this design is that the antenna doesn't cover the all the bandwidth that is specified by FCC.

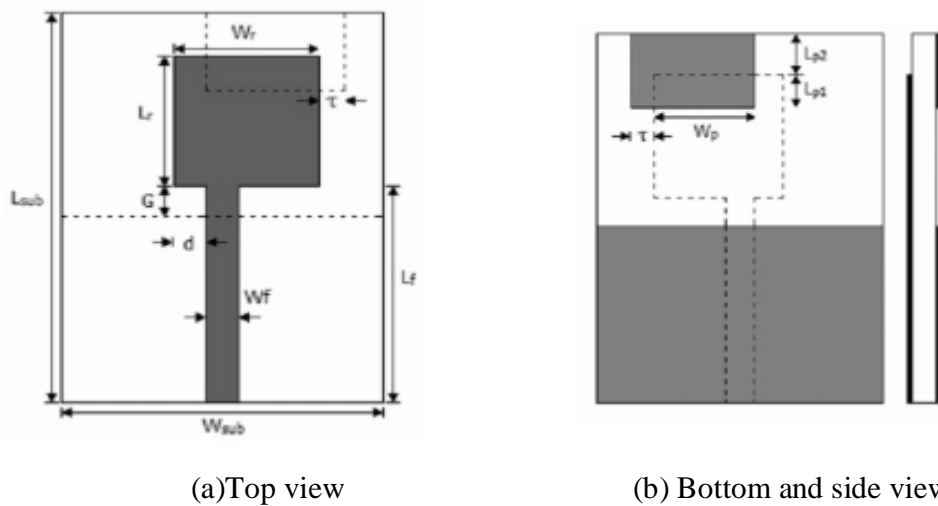


Figure (3.13): Antenna with additional external patch on back side of the substrate (a)Top view
(b) bottom and side view.

Techniques that used slotted partial ground and addition of stairs and stubs like that found in [32] caused to improved impedance bandwidth. The proposed antennas as shown in figure (3.14) have rectangular patch with slotted partial ground and two stairs at lower edge of patch and stubs at left edge of patch provide bandwidth starting from 3.2GHz to 15.7GHz. The shape of antenna is very simple and less complexity for fabrication.

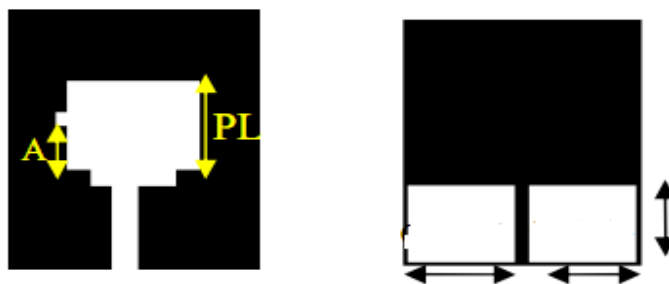


Figure (3.14): Structure of partial slotted ground antenna with addition of stair and stub.

Antenna that consists of symmetrical single-beveled planar patch with rectangular shaped slot and partial ground plane as shown in figure (3.15) are proposed on [33]. The technique used is making step at upper side of patch at both sides with horizontal slots on patch and small cut at

upper edge of ground plane provide bandwidth for this antenna start from 3.8GHz to 12GHz. The simulated result shows that the designed antenna can achieve a gain between 1.5 and 4.5 dBi against frequency which may be suitable for some application.

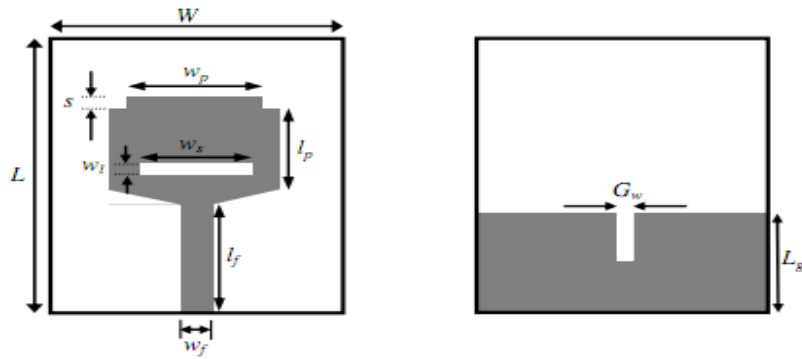


Figure (3.15): Antenna with symmetrical single-beveled planar patch with rectangular shaped slot and partial ground plane.

Technique that used Electromagnetic Band Gap (EBG) structure with microstrip antenna has been proposed in [34]. This techniques make the structure very complex for fabrication as shown in figure (3.16). This antenna is able to provide bandwidth of 4.7GHz from 5.3GHz to 10GHz which may be smaller than that specified by FCC.

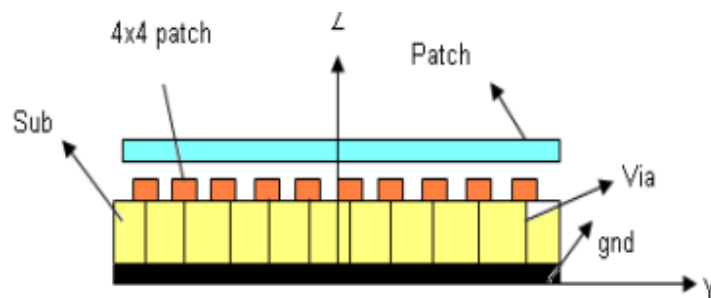


Figure (3.16): Patch antenna with EBG

Chapter 4

UWB Star Shape Antennas

4.1 Introduction

There are many different types of antennas that can be used for UWB application. Among this antenna configuration a novel design of microstrip Star Shape Antenna (SSA) is proposed. It has a simple structure and it is able to provide wide bandwidth and satisfactory radiation patterns for UWB. However, the performances and characteristics of microstrip star-shape antenna will be analyzed. In this chapter, a microstrip star-shape antenna will be studied to understand their operations.

The important parameters which affect the antenna performances will be investigated experimentally to obtain some quantitative guidelines for designing this type of antennas like, studying the effect of shifting feed line from the center of patch to the edges, in addition to the effect of changing the length of the ground plane and feed line width. Also slotted antenna with new ground plane shape which has multiple rectangular slot at top side of ground plane was investigated , and the effect of slots width and length was studied.

4.2 Antenna Structure

The structure and dimensions of the proposed antenna are given in figure (4.1). A 50Ω microstrip feed line is printed on the top of "Arlon DiClad 880 (tm)" substrate . The substrate has a thickness of $h=1.9\text{mm}$ and a relative permittivity $\epsilon_r = 2.2$. $l_s=25\text{mm}$ and $w_s=15\text{mm}$ denoting the length and width of the substrate, respectively.

The width of the microstrip feed line is fixed at $w_f=4.7\text{mm}$ to achieve 50Ω impedance. On the other side of the substrate, the conducting ground plane has a length of $l_g=7.1\text{mm}$ and width w_g is same of substrate width.

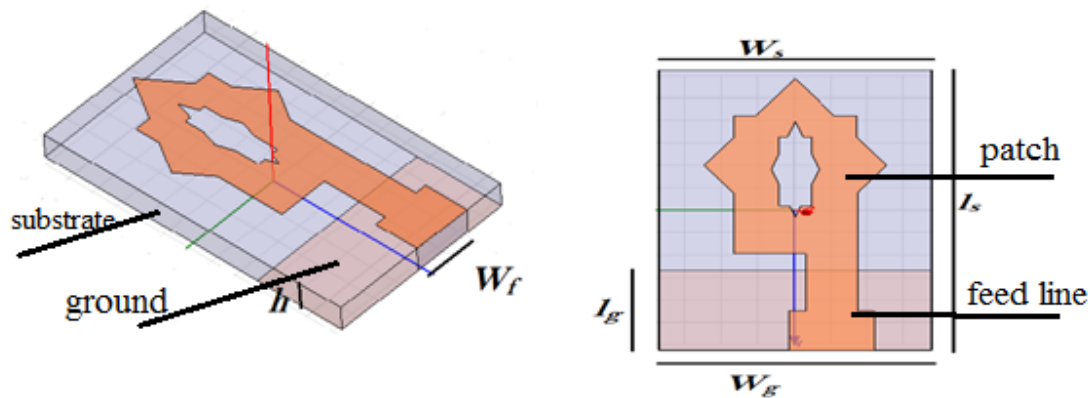


Figure (4.1): Star shaped antenna

Tables (4.1) shown below, summarized the parameter of desired antenna

Table (4.1) parameter of antenna

Width of the substrate (w_s)	15mm
Length of the substrate (l_s)	25mm
Dielectric constant of the substrate, (ϵ_r)	2.2
Characteristic impedance of feed line Z_0	50Ω
Width of Microstrip feed line (w_f)	4.7mm
Height of substrate (h)	1.9mm
Feeding method	Microstrip line feed
Length of the ground plan (l_g)	7.1mm
Frequency of operation (f)	10GHz

4.3 Simulation Setup and Result

The simulations and optimizations are based on Ansoft HFSS. HFSS is a full-wave electromagnetic simulator based on the finite element method. It has been used in several areas, like design of MICs, RFICs, patch antennas, wire antennas, and other RF/wireless antennas. It can be used to calculate and plot Return loss, VSWR, current distributions, radiation patterns, gain, input impedance etc.

4.3.1 Antenna Return loss and Bandwidth

For UWB antenna one of the most important characteristic that must be achieved is wide band.

The bandwidth of the antenna can be considered as the range of frequencies bounded by the return loss that is lower than -10dB and, it can be calculated from the return loss plot. Figure (4.2) shows that the bandwidth is covering an extremely wide frequency range start from 3.9GHz to 22.5GHz with a resonant frequency at 10.29 GHz due to good impedance matching over frequency range.

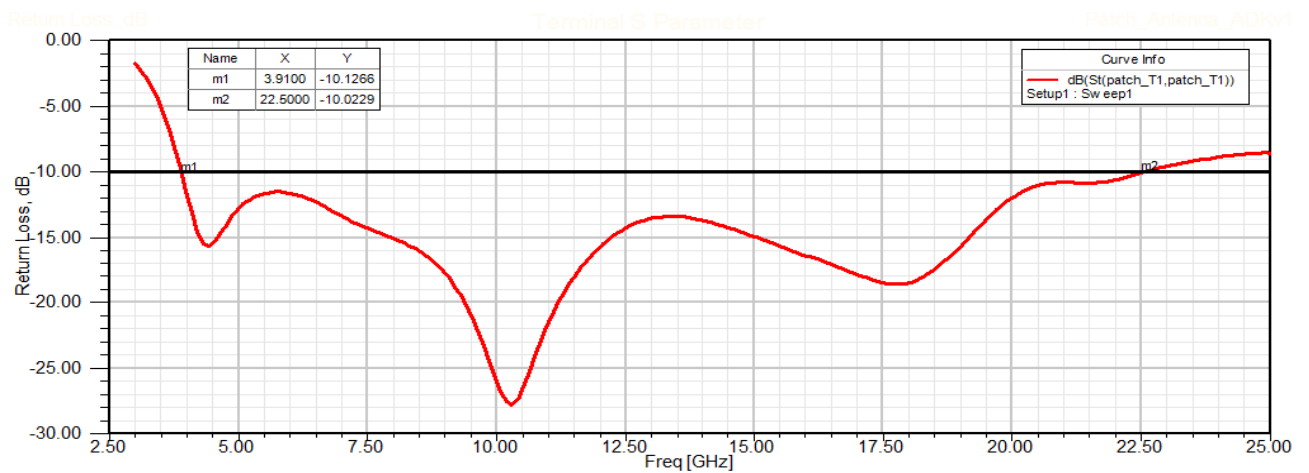


Figure (4.2): Return loss for SSA

4.3.2 Antenna Input Impedances

Antenna is usually designed to match terminal impedance of about 50Ω or 75Ω which are the common values of available coaxial cable. The microstrip transmission line was selected as a feeding technique for the desired antenna. As shown in chapter (3), in this method, a conducting

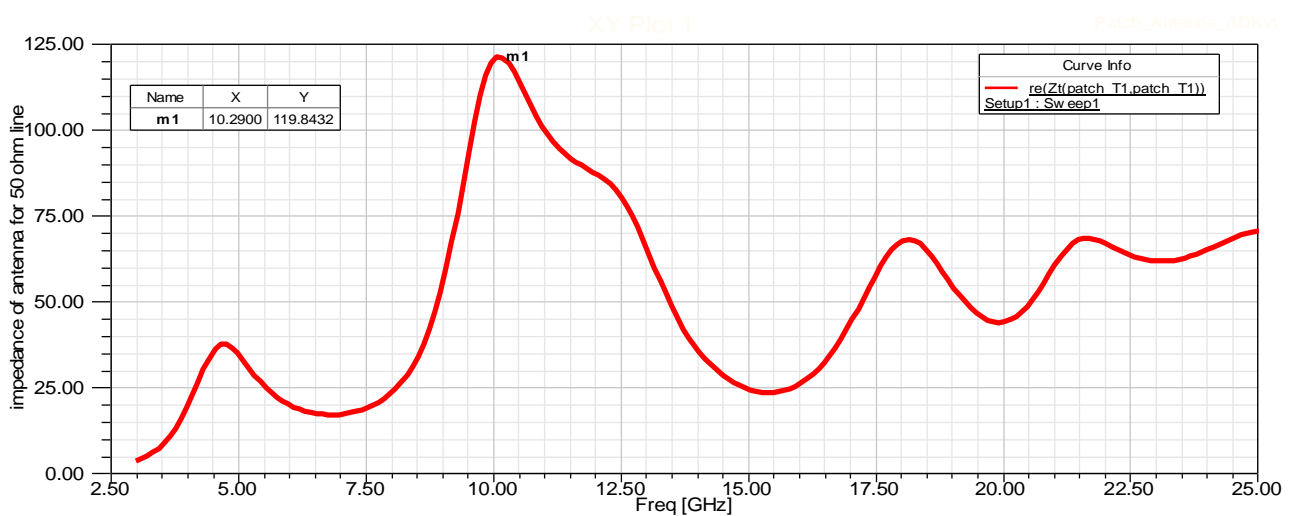


Figure (4.3):Antenna impedance

strip connects directly to the edge of microstrip patch. The advantage of this technique comes from that layout, where the feed can be etched to the same substrate to provide a planar structure. The challenge is designing a microstrip line that provides matching impedance with the antenna. For our design we used Quarter-Wavelength Transformer method to provide matching impedance. Because the shape of antenna is new and it's hard to calculate its impedance using traditional equation, we are using HFSS software to find the impedance of antenna Z_A which is 119Ω as shown in figure (4.3). This can be obtained by connecting a 50Ω microstrip line with patch as shown in figure (4.4). By using equation (2.27-2.28), we found that the width of line is equal to 5.9mm and its optimized value equal to 4.7mm as we will show later.

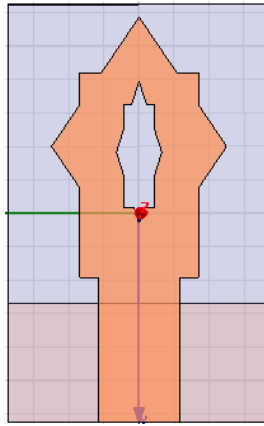


Figure (4.4): 50Ω microstrip line

Now by using equation (4.1)

$$Z_o = \sqrt{Z_A \times Z_{in}} = \sqrt{119 \times 50} = 77.3 \quad (4.1)$$

we found that the characteristic impedance is 77.3Ω , now applying equation (2.27-2.28) again to find the width of microstrip line that provides characteristic impedance equal to 77.3Ω , we found that the width is 2.88mm. So the transformer that provides matching impedance between feeding line and antenna has a length equaling to $(\lambda_g / 4)$ where λ_g is the guide wavelength and obtained from equation (2.23) which equals to 22.4 mm. So the transformer has width $w_T = 2.88\text{mm}$, length $l_T = 5.6\text{mm}$ and its optimized value using HFSS becomes equal to $l_T = 5.12\text{mm}$ and, the characteristic impedance Z_o equal to 77.3Ω , as shown in figure (4.5).

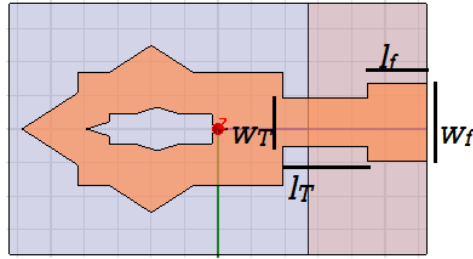


Figure (4.5): Quarter-wavelength transformer for microstrip line

Figure (4.6) shows the resistance and reactance behavior of the antenna as a function of the frequency. From the figure we see that the impedance matching is closely satisfied over the entire operational band. It shows that the return loss ($< -10\text{dB}$) always occurs over the frequency range that the input impedance is close to 50Ω , i.e. The input resistance R is close to 50Ω while the input reactance X is not far from zero. At operating frequency f , the resistance is close to 50Ω and the reactance close to 0.

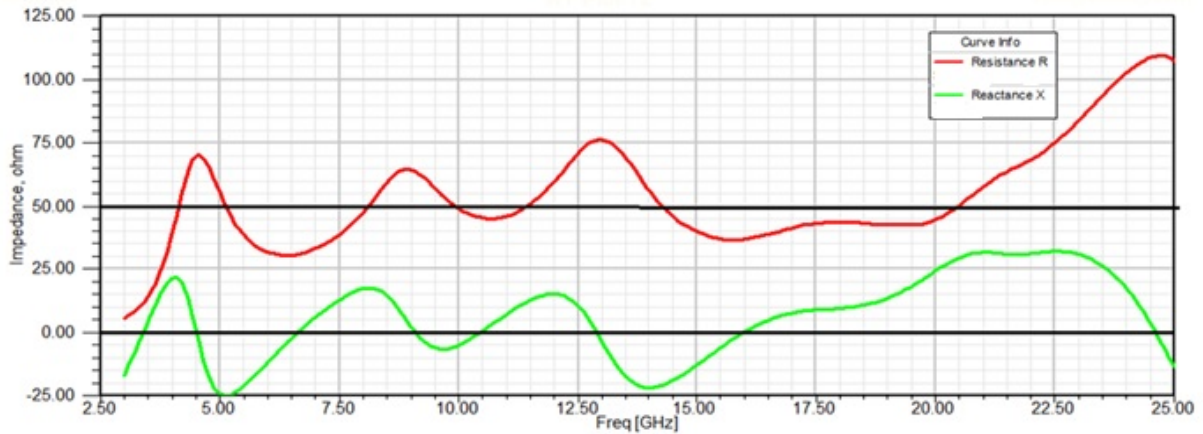


Figure (4.6): Resistance R and Reactance X.

4.3.3 Antenna Gain

The simulation of maximum gain of the optimized antenna at $\phi = 0^\circ, 90^\circ$ as a function of frequency is illustrated in figure (4.7). It shows that at 10.29 GHz and 17.8GHz frequency the gain is 4.5dB and 4.4dB respectively at $\phi = 90^\circ$ and 1.9dB, 5dB respectively at $\phi = 0^\circ$. The variation of gain over the frequency band can be explained as follow. The existence of reactive impedance as shown in figure (4.6) caused storage power and prevented it from radiating.

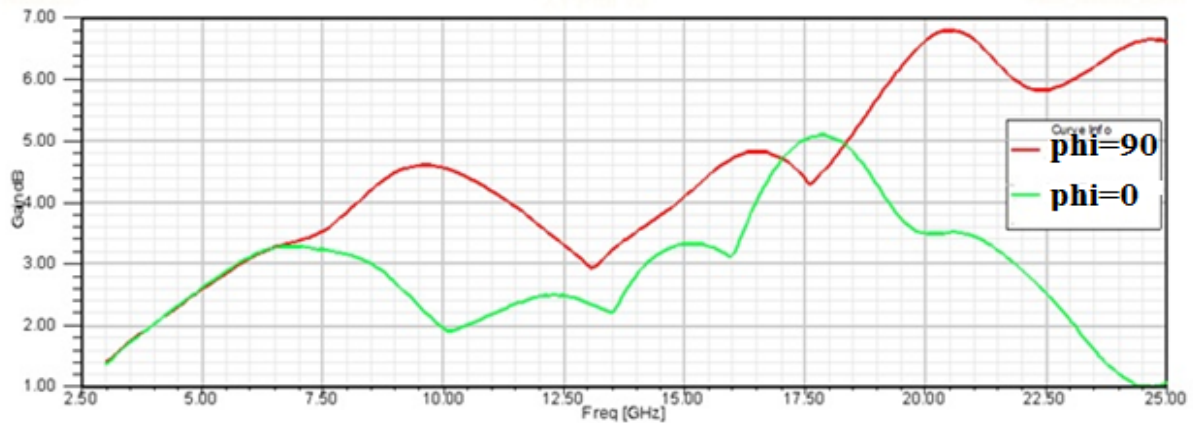
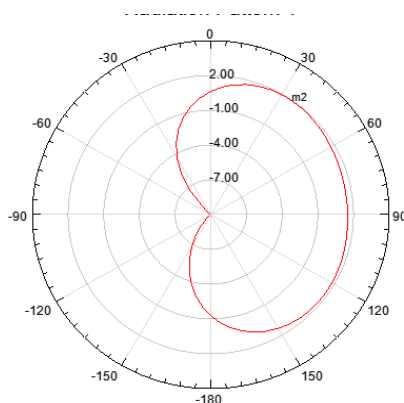


Figure (4.7): The simulated of maximum Gain at $\phi = 0^\circ, 90^\circ$ over frequency band

As the result the gain to becomes small in some ranges of frequency. Also the decrease of reactance in some range caused the power radiate more efficiently, which allows to increased gain.

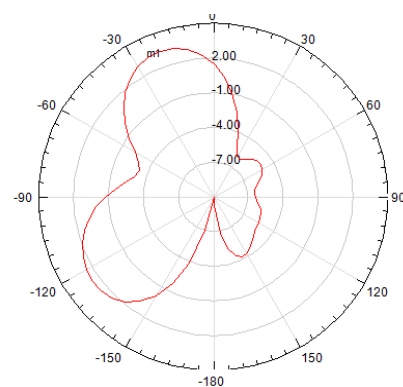
4.3.4 Antenna Radiation Pattern

Radiation pattern demonstrates the radiation properties of antenna and describes both the E and H-plane patterns. The E-plane is defined as the plane containing the electric field vector and the directions of maximum radiation while the H-plane defined as the plane containing the magnetic field vector and the direction of maximum radiation [6]. Figure (4.7) illustrates the simulated of radiation pattern for both frequency 10.29GHz and 17.8GHz at $\phi = 0^\circ, 90^\circ$ and, $\theta = 0^\circ - 180^\circ$.



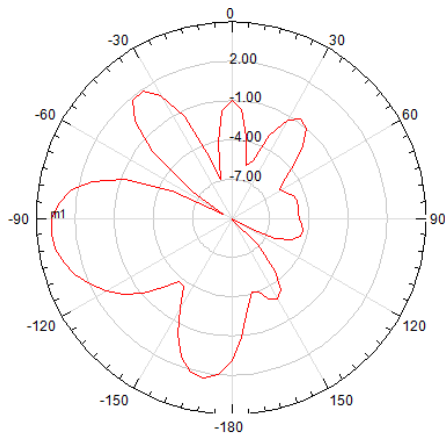
Name	Theta	Ang	Mag
m2	35.0000	35.0000	1.9526

Figure (4.7-a): E-plane at 10.2GHz, $\phi = 0^\circ$



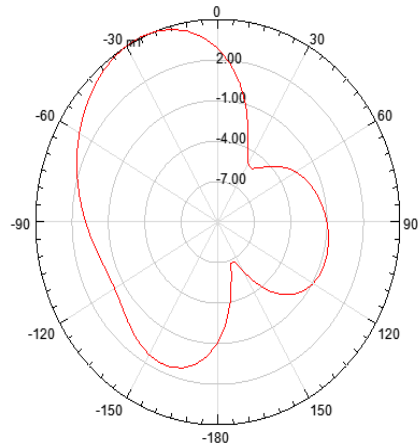
Name	Phi	Ang	Mag
m1	335.0000	-25.0000	3.2906

Figure (4.7-b): H-plane at 10.19GHz, $\theta = 90^\circ$



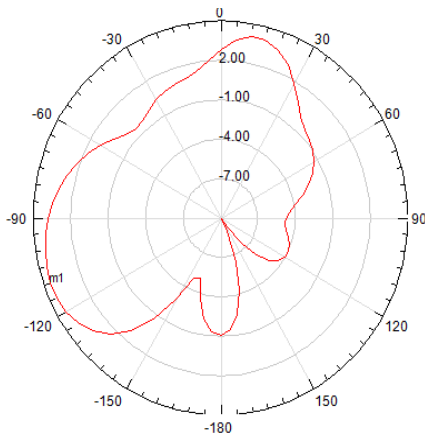
Name	Theta	Ang	Mag
m1	-30.0000	-30.0000	5.0460

Figure (4.7-c): E-plane at 17.8GHz, $\phi = 0^\circ$



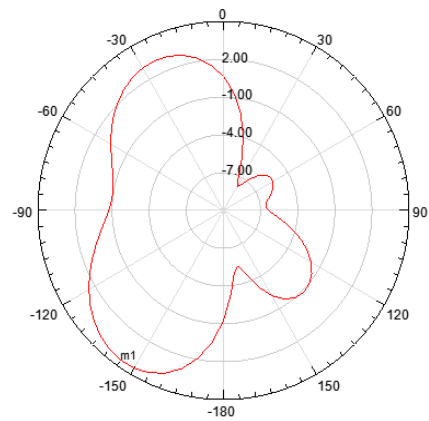
Name	Phi	Ang	Mag
m1	270.0000	-90.0000	3.7731

Figure (4.7-d): H-plane at 17.8GHz, $\theta = 90^\circ$



Name	Theta	Ang	Mag
m1	-110.0000	-110.0000	4.4600

Figure (4.7-e): y-z plane at 17.8GHz, $\phi = 90^\circ$



Name	Theta	Ang	Mag
m1	-145.0000	-145.0000	4.4831

Figure (4.7-f): y-z plane at 10.2GHz, $\phi = 90^\circ$

From figure (4.7a, b) we can notice that the radiation pattern at 10.9GHz when $\theta = 90^\circ$ H-plane is directional more than at $\phi = 0^\circ$ E-plane. This is due to the fact that the gain in H-plane is 3.2dB larger than at E-plane 1.95dB. Also from figure (4.7c-d) it is shown that the radiation pattern at 17.8GHz, when $\phi = 0^\circ$ is more directional than that at $\theta = 90^\circ$ also that the gain at is larger than at $\theta = 90^\circ$. Figure (4.7e-f) show the vertical plane of radiation pattern at $\phi = 90^\circ$ y-z plane .

4.3.5 VSWR

Voltage standing wave ratio (VSWR) of microstrip antenna shown in figure (4.8). In case of microstrip patch antenna the value of VSWR is always less than 2 [20]. At $f = 10.29$ GHz the value of VSWR is 1.01:1 and it's less than 2 over all frequency band this is due to good impedance matching which caused minimized on reflection coefficient that minimized VSWR .

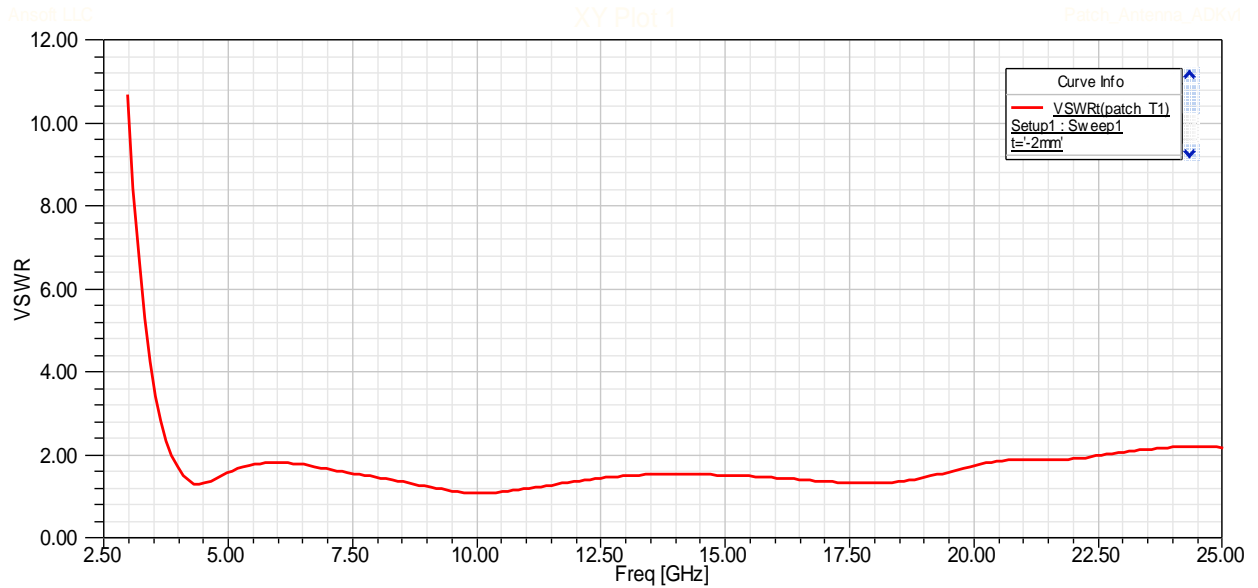


Figure (4.8): VSWR for SSA

4.4 Parameters Study

A parameter study was conducted to optimize antenna parameters. It helped to investigate the effect of different parameters on the impedance bandwidth. The effect of feed line shift of microstrip line , the ground plane length and feed line width are studied. All the antenna parameters were kept constant in the simulation except for the parameter of interest.

4.4.1 Effect of Feed Shift (Offset Feed)

Figure (4.9) illustrates the simulated return loss for different feed shift steps for microstrip line feed from the center of radiating element to its edge when the ground plan width is equal to $w_g = 15$ mm and its length is fixed at $l_g = 7.1$ mm. Shift steps $t = 0$ mm, 0.4mm, 0.8mm, 1.2mm, 1.6mm, and 2mm were simulated. It is shown in figure (4.9) that the operating bandwidth of the

antenna varies remarkably with the variation of the feed shift t . The bandwidth becomes wider when the feed line is closer to the edge of patch. The optimal feed shift is found to be 2mm with bandwidth covering an extremely wide frequency range from 3.9GHz to 22.5GHz. The resonance frequency 10.29 GHz is obtained, which is very close to the desired operating frequency. It was observed from many trials of simulations that as the feed line location is moved away from the center of the patch, the operating frequency starts to decrease and the bandwidth increase.

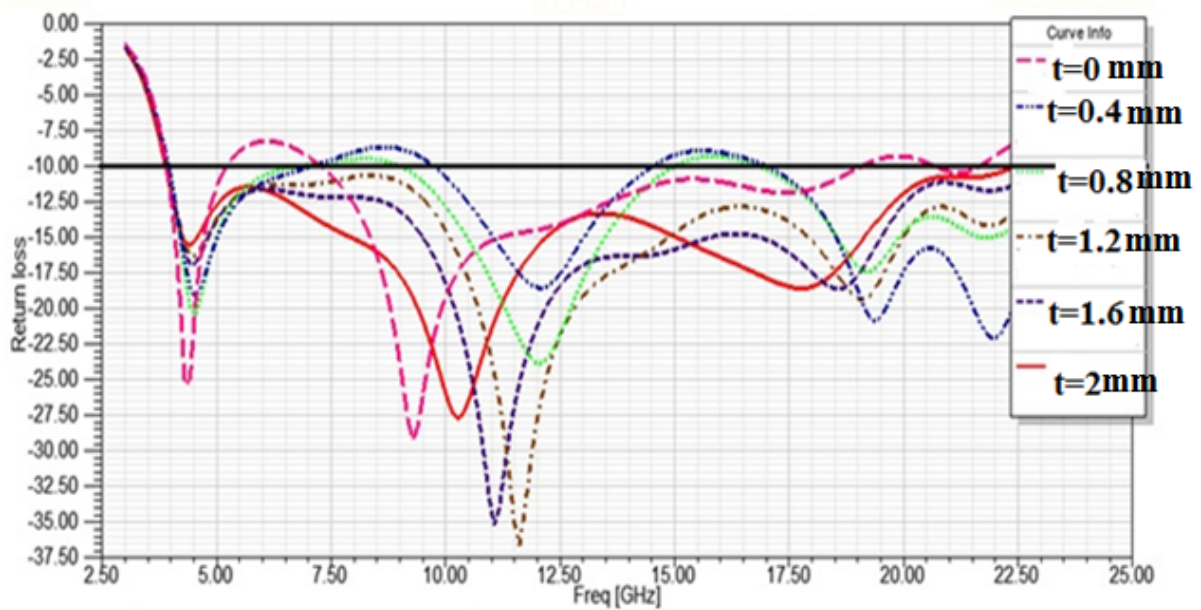


Figure (4.9): Simulated return loss curves of different feed shift

The most efficient coupling of energy are occur when the characteristic impedance of the transmission line and the terminal impedance of the antenna are the same and have no reactive components. Figure (4.10a-b) shows the variation of resistance and reactance that occurs at different feed shift steps for microstrip line, which help to explain the reason of variation of bandwidth with each feed shift step. In most of the frequency range from 3.9 to 22.5GHz, both the resistance and reactance curves fluctuate substantially. The peak value of resistance is 75Ω , while the maximum reactance is around 32Ω . When $t = 0\text{mm}$, 0.4mm , 0.8mm , resistance R change significantly at the level of 50Ω . When the return loss are close to -10dB , resistance R starts to decrease and reach a lower value, then it goes back to increase and reach a higher value. It's appears clearly at the frequency range from 5GHz to 10GHz and from 14GHz to 18.5GHz .

However, when t rises to 1.2mm, 1.6mm, and 2mm, resistance R varies more smoothly at the level of 50Ω and reactance X also fluctuates significantly across the frequency range.

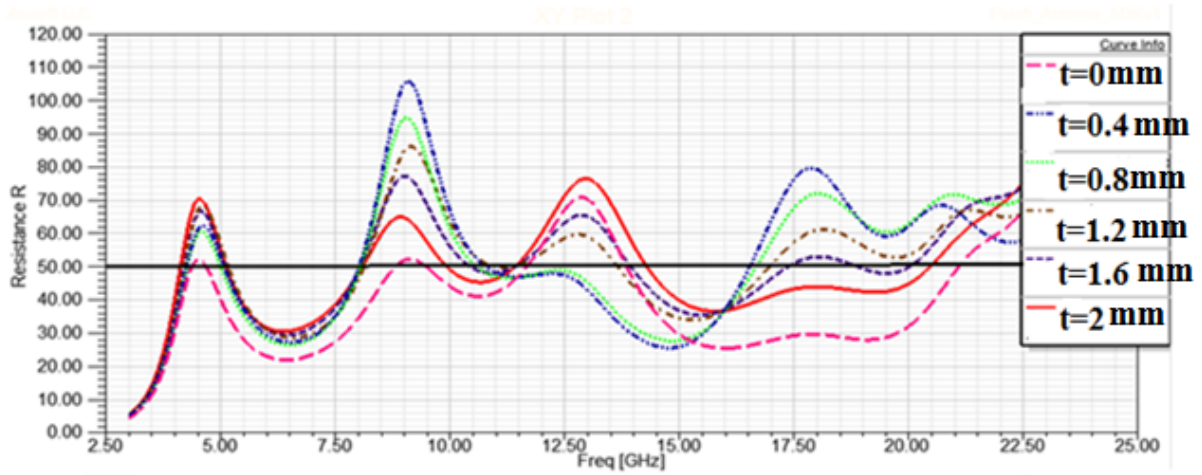


Figure (4.10-a): Resistance R

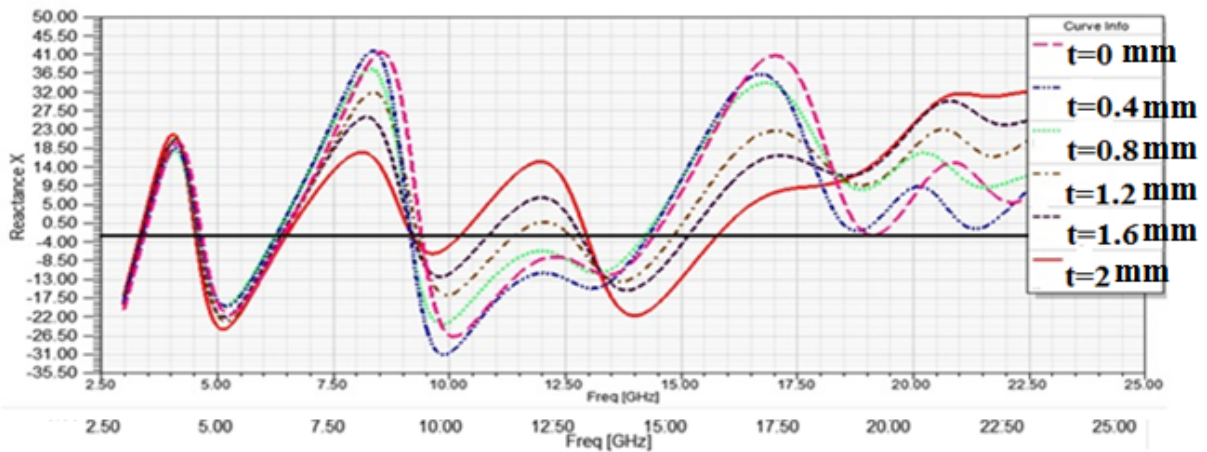


Figure (4.10-b): Reactance X

At the frequencies where resistance is close to 50 ohms, reactance is far from 0; when reactance reaches 0, resistance is either in its peak or near its minimum value. As a result, the impedance is mismatched with the antenna, leading to a narrow operating bandwidth.

The current distributions on the patch for each feed shift at a fixed ground plane length $l_g = 7.1\text{mm}$ as presented in figure (4.11). As shown in the figure, the current is mainly distributed along the microstrip feed line and the edge of the star shape of patch antenna at all feed shifts steps. At last two steps $t = 1.6\text{mm}$, 2mm the current distributed is increasing. This confirms our

previous observation that the antenna operation bandwidth are increased when the feed line becomes close to the edge of patch. Also, the electric field becomes more intense so the antenna is radiating power more efficiently due to matching impedance.

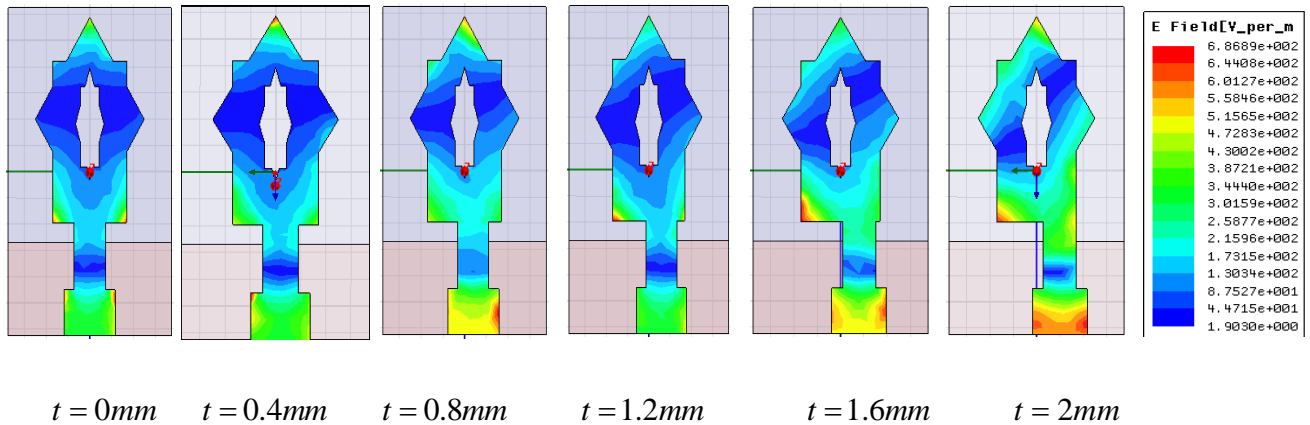


Figure (4.11): Feed shift steps for microstrip line with current distribution on patch

4.4.2 Effect of The Ground Plane Length

In previous section, it has been demonstrated that the variation of the feed shift t leads to variations of the frequency bandwidth. In a broad sense, the ground plane serves as an impedance matching circuit and also it tunes the resonant frequencies [3]. To conform this, figure (4.12) show the simulated return loss curve for the antenna with different ground lengths ($l_g = \lambda, 0.75\lambda, 0.5\lambda, 0.25\lambda$).

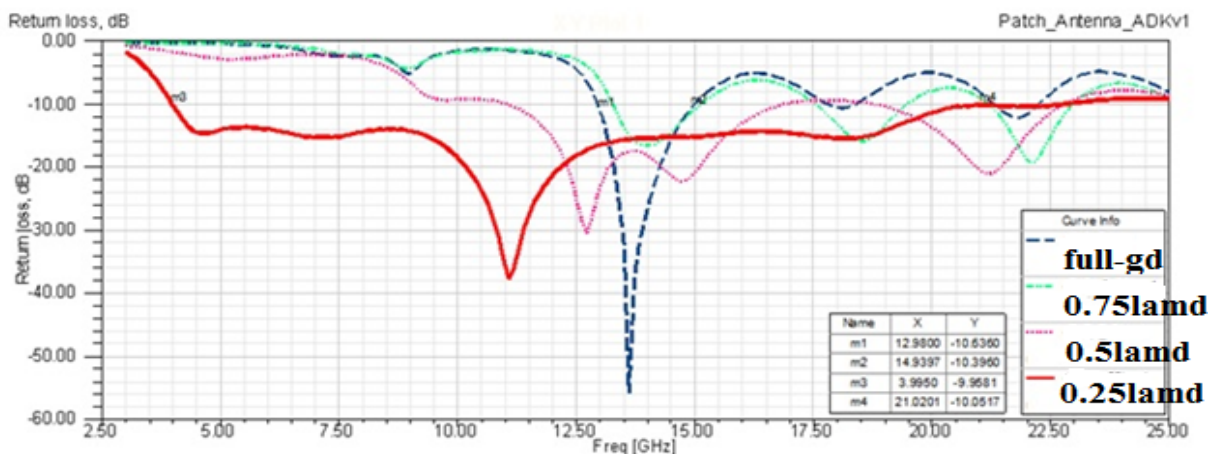


Figure (4.12): Simulated return loss curve of different ground plan length

It is noticed in figure (4.12) that at full ground plan the first-10dB bandwidth ranges from 12.9GHz to 14.9GHz, which is much narrower than that of a short ground plane. This is due to the impedance mismatch over an extreme frequency range resulting from the full ground plane. When the length of ground plane starts to decrease, $l_g = 0.75 \lambda$, 0.5λ we see that the bandwidth range starts to increase gradually and the return loss under -10dB curve becomes wider at $l_g = 0.25 \lambda$ bandwidth start from 3.9GHz to 21.GHz. The optimum values were found by optimizing the antenna is $l_g = 0.239 \lambda = 7.1\text{mm}$ were the bandwidth ranges from 3.9GHz to 22.5GHz with little frequency shift. Table (4.2) shows the value of the bandwidth at different lengths of the ground plane.

Table (4.2): show the value of bandwidth at different length of ground plane

l_g	Start frequency GHz	End frequency GHz	Bandwidth GHz
full ground plane	12.9	14.9	2
0.75λ	13.3	14.9	1.6
0.5λ	11	17.5	6.5
0.25λ	3.9	21	17.1
0.239λ	3.9	22.5	18.6

4.4.3 Effect of The Feed Line Width

Figure (4.13) shows the variation of bandwidth with the width of microstrip line. It can be

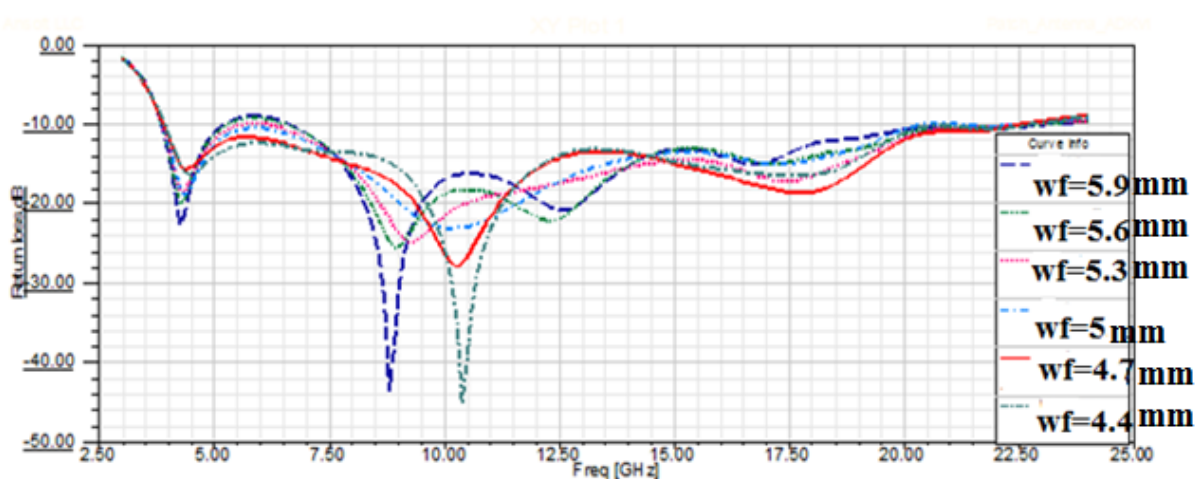


Figure (4.13): Variation of bandwidth with w_f

observed specially at lower edge of frequency. This is due to the fact that the impedance matching is very sensitive to the change of the width of microstrip line as shown in the figure (4.13). A different value of microstrip line width have been simulated ($w_f=5.9\text{mm}$, 5.6mm , 5.3mm , 5mm , 4.7mm and 4.4mm). The feed width equal to 4.7mm is found as an optimized value.

4.5 SSA with Slotted Ground Plane

As discussed in previous sections, Star Shape antenna (SSA) is capable of yielding ultra-wide bandwidth. This type of antenna is a planar structure with a microstrip feed line and a short ground plane. This section will focus on other techniques that used to enhance the bandwidth of the antenna. Other techniques have been used to enhance the bandwidth of the UWB antenna including the insertion of a modified shape in a short ground plane. Partial ground plane with multiple rectangular slot at top side as shown in figure (4.14) gives good properties for antenna that are satisfactory for UWB requirement. The antenna with new ground plane shape is the same antenna in previous section without any change on its parameters. The new ground plane shape is improving the impedance bandwidth of antenna and it's increased from 3.9GHz to 24.5GHz .

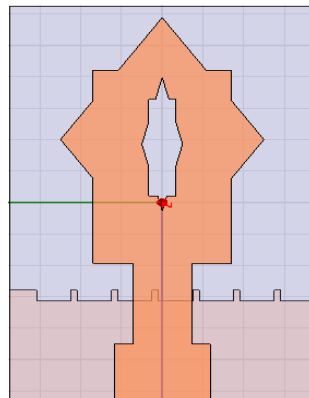


Figure (4.14): SSA with rectangular slots on ground plane

4.6 Antenna Structure

As we have shown above the (SSA) has multiple rectangular slots at top side of ground plane. Seven identical rectangular slots are embedded in the antenna's ground plane and aligned with an equal spacing 0.32mm and parallel to the patch. The embedded rectangular slots have dimension

0.67mm x1.68mm as shown in figure (4.15), this dimension is optimized using HFSS until it reaches a good result. The substrate dielectric constant are the same as used in antenna without slot "Arlon DiClad 880 (tm)" $\epsilon_r = 2.2$ " and its dimension , high ,length and, weight $h=1.9\text{mm}$, $l_s=25\text{mm}$ and $w_s=15\text{mm}$ are fixed. The modifications are insertion to the ground plane at the same length of ground plane that is used in antenna without slot $l_g=7.1\text{mm}$. The feed line is 50Ω microstrip feed line , printed on the top of substrate.

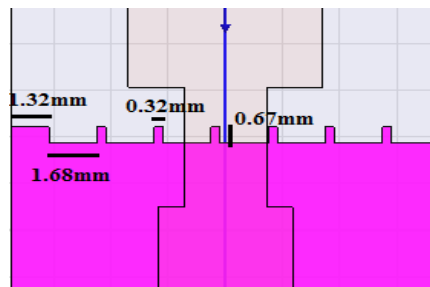


Figure (4.15): Dimension of rectangular slot

4.7 Simulation Setup and Result

The performance of the proposed antenna has been simulated and optimized by finite element method based full wave electromagnetic software Ansoft HFSS. The result and dissection are show in the coming section.

4.7.1 Antenna Return loss and Bandwidth

Figure (4.16) illustrates return loss curve for both slotted and un-slotted SSA. Its shows that the

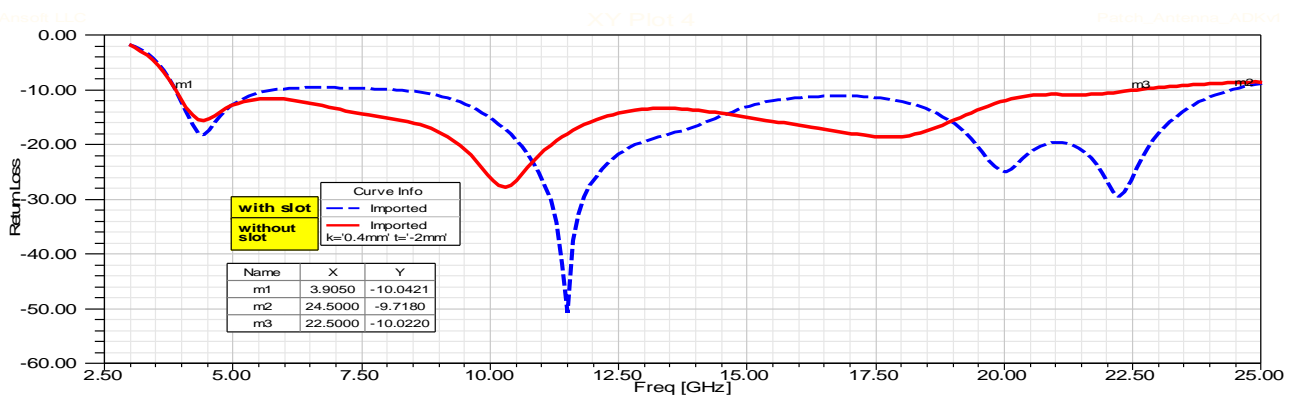


Figure (4.16):Return loss of antenna with and without slot

impedance bandwidth resulting from modified ground plane shape is covering an extremely wide frequency range from 3.9GHz to 24.5GHz with a resonance frequency at 11.5 GHz. Compare that with (SSA) in previous section the impedance bandwidth was in range from 3.9GHz to 22.5GHz and the resonance frequency is 10.29GHz, so when the proper slots are embedded in the ground plane of a microstrip antenna, the impedance bandwidth is enhanced and it becomes wider and the resonance frequency has been shifted. The slot on the partial ground plane affects the matching between radiating element and ground plane. This result in improving the bandwidth due to extra electromagnetic coupling between patch and the ground plane [29].

4.7.2 Antenna Input Impedances

A 50Ω microstrip feed line is placed on the top of substrate. The matching technique which is a Quarter-Wavelength Transformer method remains unchanged. The length of transformer is equal to $l_T=5.12\text{mm}$ with width $w_T=2.88\text{mm}$ and characteristic impedance is $77.3\ \Omega$, and $w_f=4.7\text{mm}$ which is the same dimension of antenna without slot. Figure (4.17) show the impedance behavior

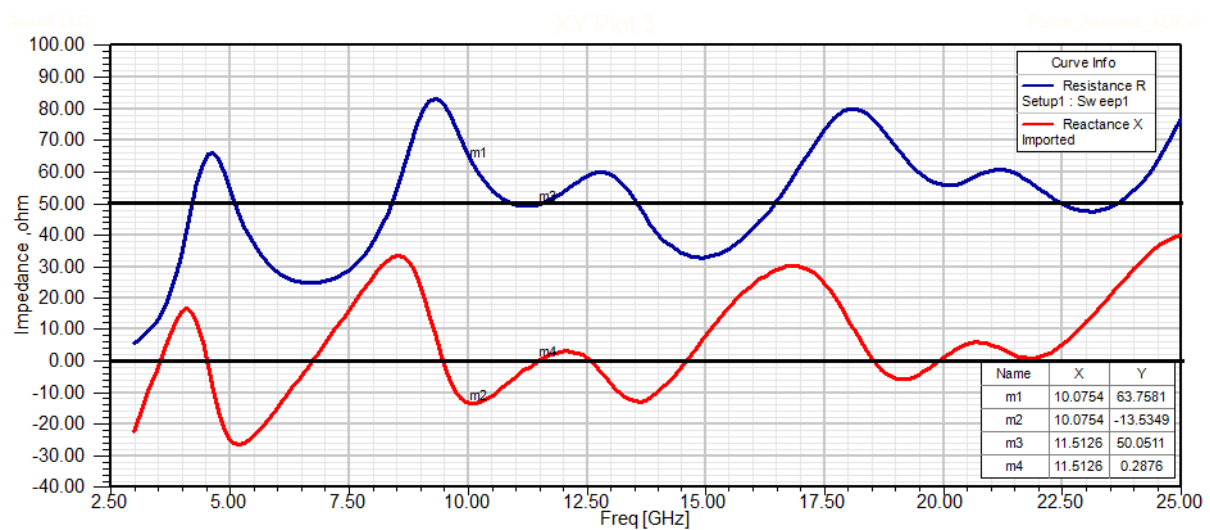


Figure (4.17): Resistance R and Reactance X

of antenna with frequency when slotted ground plane is applied .It shows that the resistance is varying between 20 Ω and 83 Ω while the reactance is changing within -26 Ω and 32 Ω throughout the impedance bandwidth. The resistance at 10 GHz is increased to 63.7 Ω and

reactance is -13.5Ω but, at new resonance frequency 11.5GHz the resistance is 50Ω and the reactance is 0Ω . From above we see that the partial ground plane serves as an impedance matching circuit and also it tunes the resonance frequencies.

4.7.4 Antenna Radiation Pattern

Figure (4.18) illustrates the simulated of radiation pattern for resonance frequency 11.5GHz in term of the E and H-plane patterns. E plane is presented by x-z plane , elevation plan, and H plane are presented by x-y plane, azimuth plane .

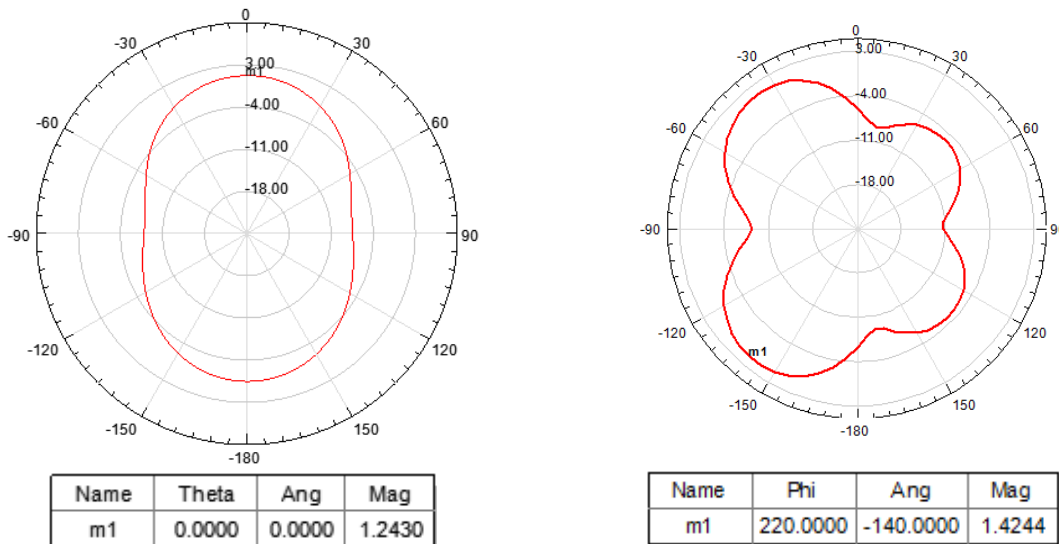


Figure (4.18-a): radiation pattern at x-z plane, $\phi=0^\circ$ Figure (4.18-b): radiation pattern at x-y, $\theta=90^\circ$

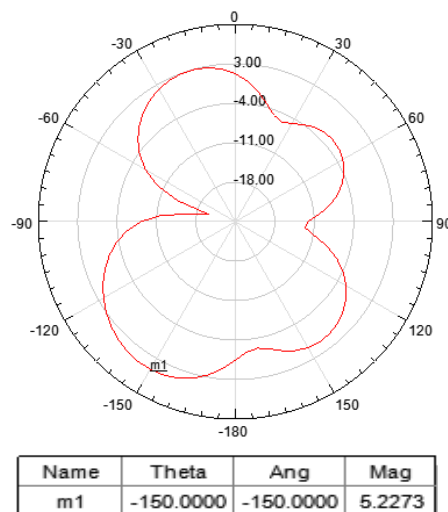


Figure (4.18-c): radiation pattern at y-z, $\phi=90^\circ$

From figure (4.18-a) we see that the radiation pattern at elevation plane x-z plane at $\phi = 0^\circ$ and θ variable are non-directional pattern and, the maximum gain is 1.2 dB at $\theta = 0, 180$ and, from figure (4.18-d) at azimuth plane x-y plane at $\theta = 90^\circ$ and, ϕ variable are directional pattern and the maximum gain is 1.42dB. The figure shows that the antenna has Omni-directional patterns. Figure (4.18-c) shows the radiation pattern in y-z plane and the maximum gain is 5.22dB.

4.7.5 VSWR

Voltage standing wave ratio (VSWR) of the microstrip antenna is shown in figure (4.19). In case of microstrip patch antenna the value of VSWR is always less than 2, so from figure (4.19) below we show that the VSWR for slotted antenna is < 2 over frequency this is due to good impedance matching which caused minimized on reflection coefficient that minimized VSWR band and this result is acceptable for many application.

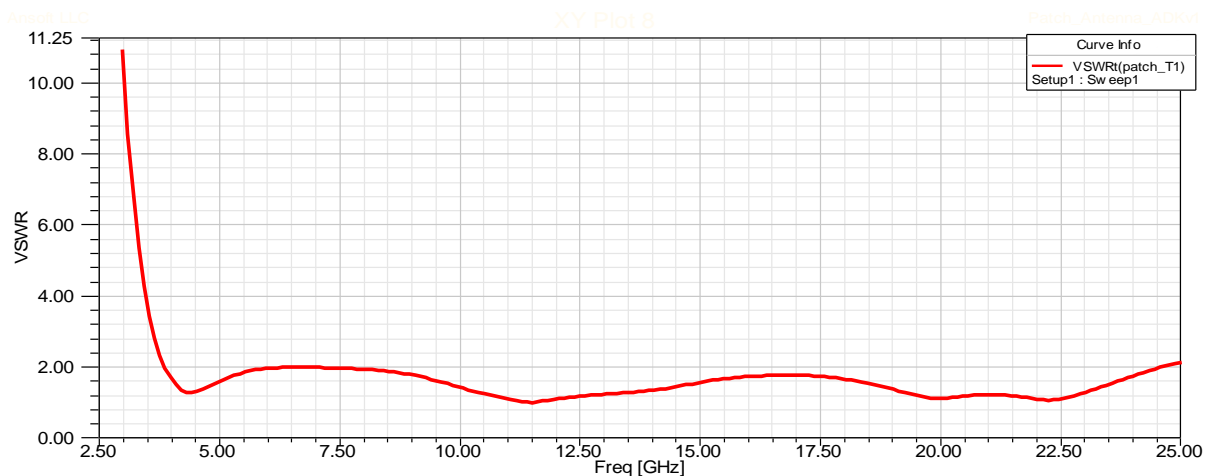


Figure (4.19): VSWR for slotted antenna

4.8 Parameters Study

Effects of slots width and length on the return loss value have been studied. Various values of both width and length of slots have been chosen. The simulated result is shown below.

4.8.1 Effect of Slots Width

Figure (4.20) shows the variation of return loss with different values of slots width ($w_s=0.42\text{mm}$, 0.84mm , 1.26mm and, 1.68mm). It can be observed that with increasing the w_s , the return loss

values are decreasing especially at upper edge frequencies of operating band and at resonance frequency 11.5GHz but at lower frequencies band it remains a little constant. This is because the impedance matching becomes enhanced at this range of frequency and so it's given better return loss value. The slot width $w_s=1.68\text{mm}$ and can be taken as the optimized value that gives better return loss value.

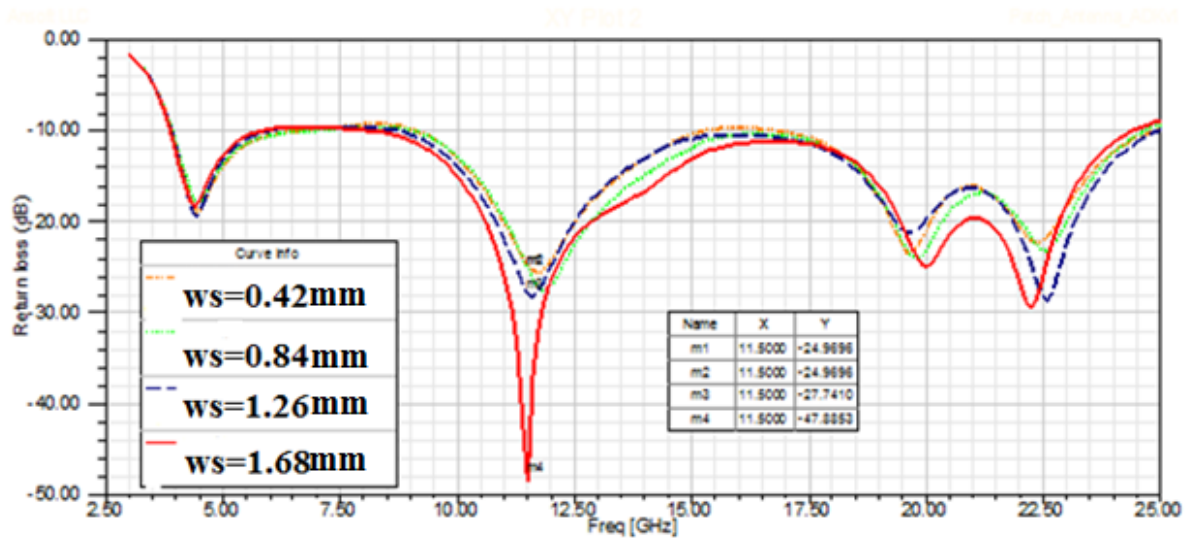


Figure (4.20):Variation of RL with for different ($w_s=0.42\text{mm}$, 0.84mm , 1.26mm and, 1.68mm)

Table (4.3) below shows the different value of return loss with different slots width at resonance frequency 11.5GHz.

Table (4.3) value of return loss at 11.5GHz with different slots width

#	slots width (w_s , mm)	Return Loss (dB)
1	0.42mm	-24.9
2	0.84mm	-24.9
3	1.26mm	-27.7
4	1.68mm	-47.8

4.8.1 Effect of Slots Length

The variation of return loss with different value of slots length ($l_s=0.167\text{mm}$, 0.334mm , 0.501mm and, 0.67mm) can be demonstrates from figure (4.21) below while the other parameters are fixed. It can show that with increasing the slots length the return loss values are

increased especially at upper frequencies band for $l_s=0.167\text{mm}$, 0.334mm and, 0.501mm . At lower frequencies band it also remains a little constant. Again with increasing the slots length l_s , the impedance matching become poor at higher frequency .So we can note that the length of slots have opposite effects of the width at upper edge of frequency band in return loss value. The better value of slots length can be found at $l_s= 0.67\text{mm}$.

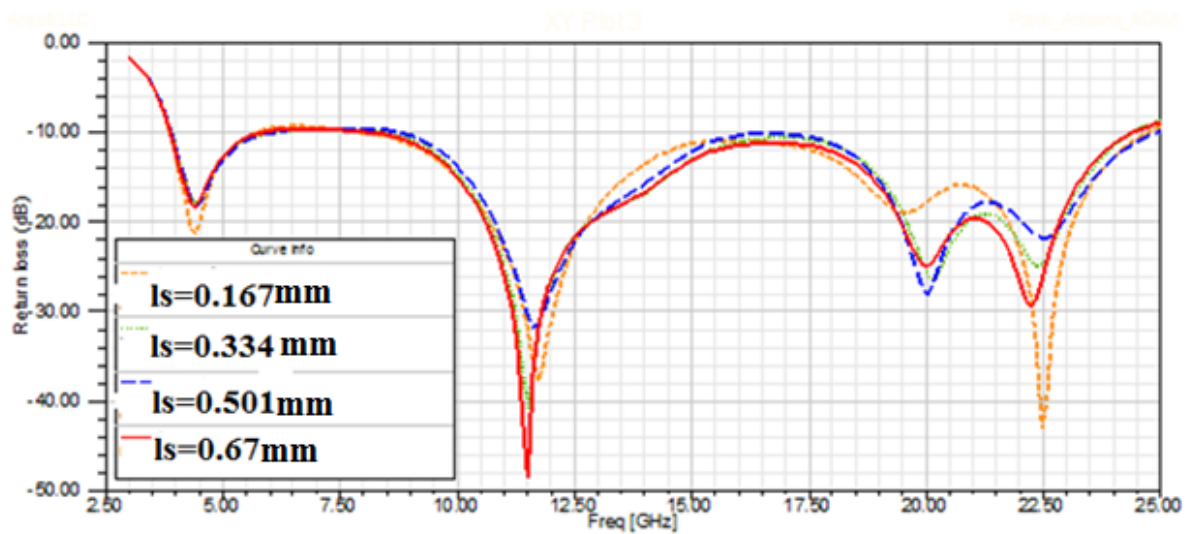


Figure (4.21):Variation of RL with different ($l_s=0.167\text{mm}$, 0.334mm , 0.501mm and, 0.67mm)

Chapter 5

Conclusions and Future Work

5.1 Conclusion

Designing UWB antenna is the main challenge in wireless communication system applications due to bandwidth requirements. In this thesis, a design of a new microstrip UWB antenna with good performance was proposed. The antenna was designed and simulated using Ansoft's HFSS electromagnetic simulation package. Two types of microstrip antennas have been designed and studied.

The first antennas the microstrip Star Shaped Antenna (SSA). This antenna provides good UWB properties, UWB impedance bandwidth from 3.9GHz to 22.5GHz and gain variation from 1.9dB to 6.9dB over the frequency of operation. The feeding used is microstrip line and quarter-wavelength transformer was used for matching.

Various parameters of antenna such as impedance matching, radiation pattern, and VSWR were studied. The impedance bandwidth enhancement techniques were used. Shifting the feed line from the center of patch to its edge was studied and the effect of bandwidth enhancement was shown. Also truncation of the ground plan method was studied, and the effect of varying feed line width was investigated.

The second antenna is SSA with slots and new short ground plane was proposed. A multiple rectangular slots at top side of the ground plane are used to enhance the impedance bandwidth of antenna. The antenna used is the star-shaped antenna without any change in the parameters. The impedance bandwidth of antenna was improved and its cover range from 3.9GHz to 24.5GHz. The other parameter of antenna like impedance matching, radiation pattern, and VSWR were

given. Also the effect of length and width of slots was studied and we conclude that the length of slots has opposite effects on the width at upper edge of frequency band in return loss value.

5.2 Suggestions for Future Work

Based on the conclusions drawn and the limitations of the work presented, future work can be carried out in the following areas:

- At present facility for fabrication of patch antenna is not available in our university; the same work will be performed later. The simulated, optimized and experimental results will be compared.
- As has been shown for both antennas, the work was concentrated on how to improve the impedance bandwidth. So, the future work may have its gain improved in order to enhance the quality of the communication link and improve channel capacity and range, directional systems with high gain are required for some applications.
- In our work here we used Quarter-Wavelength Transformer method to provide impedance matching, inset feed method may be used and the results should be compared show result.
- Microstrip transmission line was used as feed line, other feeding techniques like, coaxial cable, Aperture-coupled feed and, Proximity Coupled Feed may be used.
- The bandwidth of both antenna starts from 3.9 GHz, starting at 2 GHz could be studied to include Wi-Fi and Bluetooth application .

References:

- [1]H.N. Author and ,R.P. writer, "Introduction to Ultra Wideband for Wireless Communications",2009, Springer Science
- [2]H.G. Author, "a Brief History of UWB Antennas", in IEEE UWBST Conference, Copyright © 2003 IEEE.
- [3]J.L. Author , "Antenna Study and Design for Ultra Wideband Communication Applications", a thesis submitted of Doctor of Philosophy, University of London, United Kingdom, July 2006.
- [4]B.A. Author et al.," Ultra Wideband Applications, Technology and Future perspectives", International workshop on convergent technologies (IWCT), 2005.
- [5]J., Z. Q. Author et al, "A Compact Linear Tapered Slot Antenna With Integrated Balun For UWB Application", Progress In Electromagnetic Research C, Vol. 29, 163176, 2012.
- [6] *Antenna Theory Analysis and Design*, third edition , ohn Wiley & Sons, Inc , Canada, 2005.
- [7]C.Y. Author , " Active Microstrip Array Antennas", Submitted for the degree of Bachelor of Engineering, University of Queensland, October 2000.
- [8] (2012, Oct 11) [Online]. Available <http://www.me.berkeley.edu/ME280A/chapter1.pdf>
- [9] *CAD of Microstrip Antenna for Wireless Application* ", Artechhous, london.
- [10]Chad Orzel , July 23, 2007.Basic Concepts: Polarization of Light [Online]. Available: <http://scienceblogs.com/principles/2007/07/23/basic-concepts-polarization-of>.
- [11]*Broadband Microstrip Antennas*, Girish Kumar and, K. P. Ray, , Artech House, Boston London,2003.
- [12]Peter J. Bevelacqua .Microstrip Patch Antennas. (2012, Oct 28) [Online]. Available:<http://www.antenna-theory.com/antennas/patches/antenna.php#introduction>
- [13]D. Orban and G.J.K. Moernaut.The Basics of Patch Antennas Orban Microwave Products (2 012, may 2) [Online]. Available:www.orbanmicrowave.com .
- [14]Y. C. Author, "Analysis of Dual Band Rectangular Microstrip Antenna Using IE3D/PSO",A Thesis submitted for the degree of mater of technology, Department of Electronics and Communication Engineering, National Institute of Technology,2009.
- [15](2012,may2)[online].Available.<http://www.csus.edu/indiv/o/oldenburgj/EEE244/Chapter2/MicrostripDesCompl.pdf>

- [16] *Modern Antenna Design*, Tomas A. Milligan, ", Second Edition, John Wiley & Sons, 2005
- [17] Peter J. Bevelacqua, *Transmission Lines* (2012, sept, 2) [online]. Available : <http://www.antenna-theory.com/antennas/patches/patch3.php>
- [18] Peter J. Bevelacqua, *Transmission Lines: Quarter-Wave Transformer* (2012, sept, 2) [online]. Available . <http://www.antenna-theory.com/tutorial/txline/transmission5.php>
- [19] X. H. Author et al, " Note on Antenna Design in UWB Wireless Communication System ", in National University of Singapore
- [20] Y.D. Author and A.N. writer , "UWB Antennas: Design and Modeling", Grenoble Institute of Technology France.
- [21] W. W. Author et al, " Basic Properties and Design Principles of UWB Antennas ", *Proceedings of the IEEE*, Vol.97, No.2, February 2009 .
- [22] *Numerical Techniques in Electromagnetic* , Matthew N. O. Sadiku ,", Second Edition, CRC Press LLC, 2000, Florida.
- [23] *Electromagnetic field theory for physicists and engineers Fundamentals and Applications* R. Gómez Martín ,.
- [24] *The Finite Element Method and Applications in Engineering Using ANSYS* , E.M. and, I. G. The University of Arizona, Springer Science-n Business Media, LLC, 2006.
- [25] *Finite Element Method Magnetics* , David Meeker, October 16, 2010.
- [26] K.-S. Author et al , "Design and construction of microstrip UWB antenna with time domain analysis" 2008
- [27] S. H. Author et al "A New Ultra Wide Band antenna for UWB application", Department of Radio Wave Engineering Hanbat National University, 4 August 2003.
- [28] M. Y. Author et al, "Design and Implementation of a Novel Planer UWB Monopole Antenna for Multipath Environments ", 13th International Conference on ,ASAT- 13, May 26 – 28, 2009.
- [29] M. T. Author et al, "Design and optimization printed rectangular antenna for UWB application " , *World applied sciences journal* 10, 2010.
- [30] L. C. Author et al, " Enhanced Bandwidth of Impulse-Ultra Wideband (I-UWB) Slotted Rectangular Patch Antenna with Partial Ground Plane" , *IJECCT* 2010.
- [31] M.G. Author and M. Y. Writer, "" Bandwidth Enhancement Techniques Comparison for Ultra Wideband Microstrip Antennas for Wireless Application " in *Journal of Theoretical and Applied Information Technology*, January 2012.

[32]I.R. Author et al.," Design of Microstrip Patch Antenna Using Slotted Partial Ground And Addition Of Stairs And Stubs For UWB Application", in Multidisciplinary Journals in Science and Technology, Journal of Selected Areas in Telecommunications (JSAT), May Edition, 2012

[33]B.K. Author et al.," A Compact Microstrip Antenna for Ultra Wideband Applications ", in European Journal of Scientific Research,2011.

[34] A.A. Author and Y. Writer," Electromagnetic Band Gap Coupled Microstrip Antenna for UWB Applications ", in IOSR Journal of Electronics and Communication Engineering, (Sep-Oct 2012